

# Supporting Information

In the following sections, we present both analytical arguments based on the mathematical models and additional computational results that support the main results of the study. Sections 1 to 5 contain analysis of the well-mixed configuration. Section 6 describes the model used to examine the effect of resource competition between nodes (also examined in a well-mixed configuration). Sections 7 to 12 cover the uniform 1-D channel, with sections 7 to 8 covering the basic aspects and the remaining sections covering localised bistable and oscillatory circuits.

## Summary of sections

### 1. **Steady state analysis of the well-mixed configuration**

Here we present the basic steady state aspects of a basic scenario - a two compartment system with gene expression in one of the compartments. We explain how a simplified compartmental description is obtained at steady state from the full PDE model. Such descriptions are used for further analysis in the following sections.

### 2. **Analysis of non-monotonic variation of steady state concentrations**

Here we present analytical results for the well-mixed configuration, that demonstrate how steady state concentrations in a given compartment can vary non-monotonically in response to variation in compartment separation.

### 3. **Two-node mutual inhibition motif: Simplified model**

Here we present the simplified description used to generate the two parameter bifurcation diagrams presented in the text for the two-node mutual inhibition circuit. We also use this model to elucidate the effect of modular augmentations to a configuration.

### 4. **Localizing a bistable motif: Well-mixed compartments**

Here we analyse the basic effects of localising a single node bistable circuit (as used by (Gines et al. 2017)) in a configuration of well mixed compartments. We analyse the effect of placement in a linear array of compartments, as well as separating the degrading enzyme from the circuit.

### 5. **Adaptation to spatial separation**

Here we present analytical results that demonstrate how steady state concentration of a protein in a given compartment can be made to adapt to changes in spatial separation, by negative regulation. We also demonstrate how this feature can be combined with adaptation to template amounts.

### 6. **Effect of competition for resources - Fixed total RNAP**

Here we present details of the model used to examine the effects of competition for resources between two gene-expression nodes.

### 7. **Single production compartment in a uniform channel**

Here we present analytical results for a single compartment in a channel configuration - steady state profiles for different boundary conditions. We also discuss adaptation to spatial separation in a uniform channel. We also demonstrate the possibility of finding alternative locations that maintain interaction strengths between nodes.

### 8. **Effect of membranes bounding compartments**

Here we present a brief discussion of how membranes bounding compartments may affect our conclusions, and how they may be incorporated within our framework.

### 9. **Spatial organisation of degradation**

Here we present analytical results for the 1-D channel, that we use to demonstrate the effect of different ways of distributing the degrading enzyme.

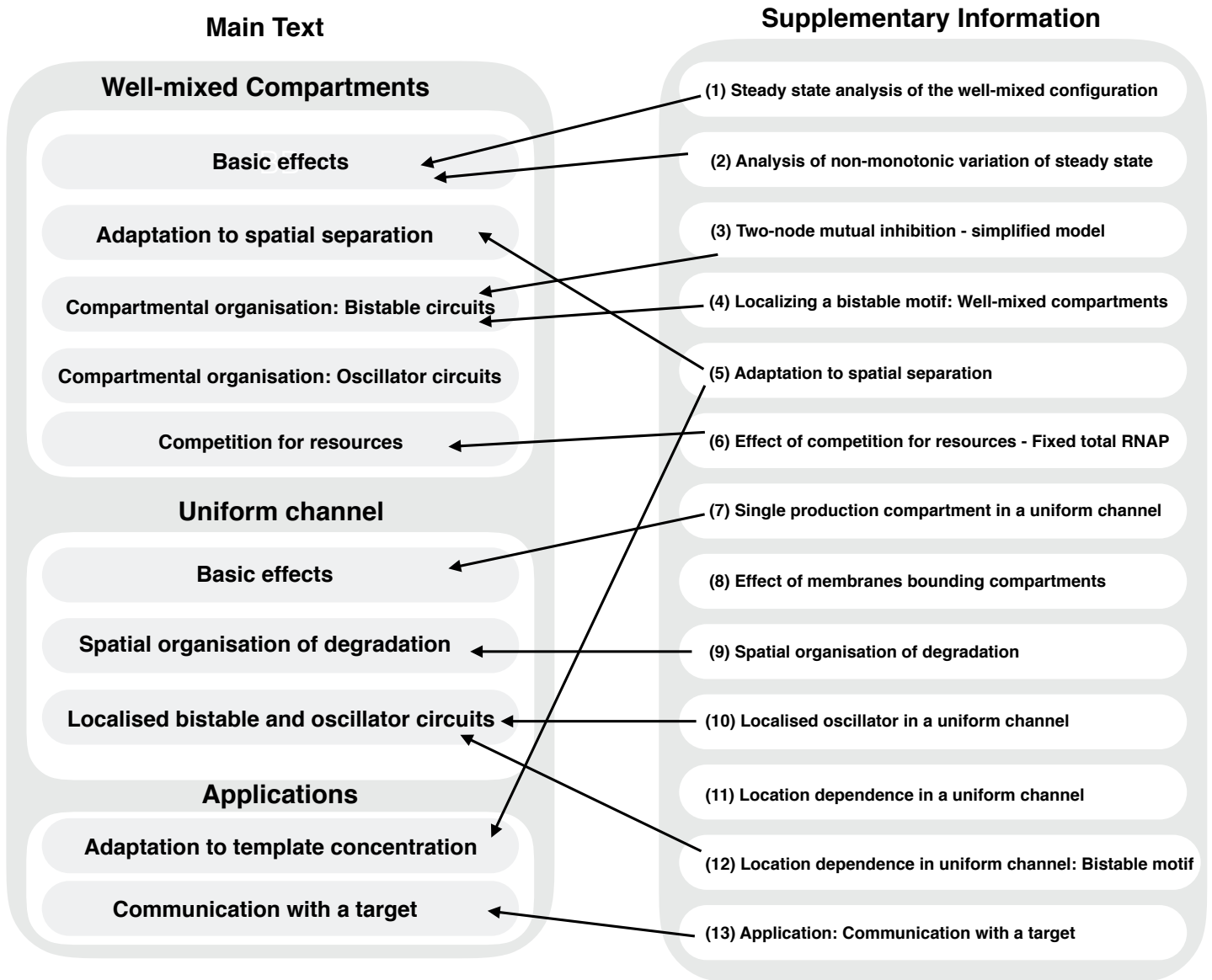


**Figure S0:** Schematic of the organisation of the paper and the supporting information. The arrows indicate which sections of the supporting information contain analysis and discussion pertaining to the results presented in each of the sections in the main text.

**Figure S00:** Schematic layout of results in the paper

### Well-mixed Compartments

**Basic effects: Leaks and compartment separation**

**Consequences for feedback**

**Appealing feature: Adaptation to spatial separation**

**Compartmental organisation: Bistable circuits**

**Compartmental organisation: Oscillator circuits**

**Competition for resources**

### Uniform Channel

**Effect of open boundaries** (no degradation)

**Symmetric locations for sender-receiver systems**  
(Including uniform degradation)

**Spatial organisation of degradation**

**Localised bistable and oscillator circuits**

### Exemplar problems

**Adaptation to template concentration**

**Communication with a target**

## 10. Localised oscillator in a uniform channel

Here we present the model of the PEN toolbox based oscillator (as used by Genot et al. (2016)) that we use to examine the effect of localisation in a 1-D channel. We also discuss similar effects seen in the activator inhibitor TX-TL oscillator examined in our study, as well as in other models of chemical oscillators in the literature.

## 11. Location dependence in a uniform channel: Single production compartment

Here we present analytical results that demonstrate the basic location dependent behaviour of steady state profiles for a single production compartment in a 1-D channel with both open and closed boundaries.

## 12. Location dependence in a uniform channel: Localizing a bistable motif

Here we build on the analysis in the previous section to demonstrate the possibility of location dependent bistable characteristics for a bistable circuit localised in a 1-D channel with closed or open boundaries.

## 13. Application: Communication with a target

Here we present analytical results for the prototypical scenario of distributed circuit design presented in Figure 7.

# Contents

<b>1</b>	<b>Steady state analysis of the well-mixed configuration</b>	<b>3</b>
<b>2</b>	<b>Analysis of non-monotonic variation of steady state concentrations</b>	<b>5</b>
2.1	Activation - Monomeric regulation . . . . .	5
2.2	Activation - Dimeric regulation . . . . .	6
2.3	Repression - Monomeric regulation . . . . .	7
2.4	Repression - Dimeric regulation . . . . .	8
2.5	Mutual-activation motif: effect of spatial separation . . . . .	8
<b>3</b>	<b>Two-node mutual inhibition motif: Simplified model</b>	<b>9</b>
3.1	Modular Augmentation . . . . .	10
<b>4</b>	<b>Localizing a bistable motif: Well-mixed compartments</b>	<b>10</b>
4.1	Spatial Separation of the degrading enzyme . . . . .	11
4.2	Placement in a linear array of compartments . . . . .	11
4.3	Localizing the two node mutual inhibition motif . . . . .	12
<b>5</b>	<b>Adaptation to spatial separation</b>	<b>13</b>
5.1	Two compartment configuration: X and Y apart . . . . .	14
5.2	Two compartment configuration: X and Y co-localised . . . . .	15
5.3	Effect of additional upstream regulation of X . . . . .	16
5.4	Three compartments: Case 1 . . . . .	16
5.5	Three compartments: Case 2 . . . . .	17
5.6	General case . . . . .	19
5.7	Dimeric regulation . . . . .	20
5.8	Adaptation to template concentrations . . . . .	21
5.9	Exemplar case: combined adaptation to template concentration and spatial separation . . . .	23
<b>6</b>	<b>Effect of competition for resources - Fixed total RNAP</b>	<b>23</b>

<b>7</b>	<b>Single production compartment in a uniform channel</b>	<b>24</b>
7.1	Open boundaries and no degradation . . . . .	24
7.2	Closed boundaries and uniform degradation . . . . .	25
7.3	Open boundaries and uniform degradation . . . . .	26
7.4	Adaptation to spatial separation in the uniform channel . . . . .	27
7.5	Finding symmetric locations . . . . .	27
<b>8</b>	<b>Effect of membranes bounding compartments</b>	<b>28</b>
<b>9</b>	<b>Spatial organisation of degradation</b>	<b>28</b>
9.1	Systems insights applied to a bistable circuit - adaptation to spatial separation . . . . .	30
<b>10</b>	<b>Localised oscillator in a uniform channel: ‘Predator-Prey’ Oscillator</b>	<b>30</b>
<b>11</b>	<b>Location dependence in a uniform channel: Single production compartment</b>	<b>31</b>
11.1	With open boundaries and no degradation . . . . .	31
11.2	With closed boundaries and uniform degradation . . . . .	32
<b>12</b>	<b>Location dependence in a uniform channel: Localizing a bistable motif</b>	<b>33</b>
12.1	Placement in an open domain . . . . .	33
12.2	Placement in an closed domain with uniform degradation . . . . .	34
<b>13</b>	<b>Application: Communication with a target</b>	<b>35</b>
<b>14</b>	<b>Retroactive effect in a uniform 1-D channel:</b>	<b>36</b>
<b>15</b>	<b>Parameters</b>	<b>37</b>
15.1	Spatial Parameters . . . . .	37

## 1 Steady state analysis of the well-mixed configuration

The basic models used for transcription-translation circuits throughout the study include the formation of protein dimers. While dimerisation plays an important role in those cases where we focus on nonlinear behaviour - bistability and oscillations - it does not always introduce qualitative differences to the results obtained in relation to simpler circuits and basic effects. In cases where it does introduce qualitative differences, we mention this in the text.

The basic model for a transcription-translation circuit is as follows. The diffusivity and rate constant of leak/degradation are assumed to be equal for both monomeric and dimeric forms. Dimerisation is assumed to occur wherever the protein monomer is present (i.e. both in the compartments and in the connecting channels). For a two compartment configuration (equal sized compartments), the model equations for a protein X, whose expression is regulated by the dimer form of a protein Y, are (similar to Karzbrun et al.

(2014)) given as:

In compartment 1 ,

$$\begin{aligned}\frac{dP_X}{dt} &= k_X^b Y_{dim}(P_X^T - P_X) - k_X^u P_X \\ \frac{dM_X}{dt} &= r_X^c(P_X^T - P_X) + r_X^y P_X - r_X^d M_X \\ \frac{\partial X}{\partial t} &= k_X^t M_X - 2k_X^2 X^2 + 2k_X^{-2} X_{dim} - k_X^d X + D_X \frac{A}{V} \left( \frac{\partial X}{\partial \theta} \right)_{\theta=0} \\ \frac{\partial X_{dim}}{\partial t} &= k_X^2 X^2 - k_X^{-2} X_{dim} - k_{X_2}^d X_{dim} + D_{X_{dim}} \frac{A}{V} \left( \frac{\partial X_{dim}}{\partial \theta} \right)_{\theta=0}\end{aligned}$$

Between compartments ( $\theta \in [0, L]$ ),

$$\begin{aligned}\frac{\partial X}{\partial t} &= -2k_X^2 X^2 + 2k_X^{-2} X_{dim} + D_X \frac{\partial^2 X}{\partial \theta^2} \\ \frac{\partial X_{dim}}{\partial t} &= k_X^2 X^2 - k_X^{-2} X_{dim} + D_{X_{dim}} \frac{\partial^2 X_{dim}}{\partial \theta^2}\end{aligned}$$

In compartment 2 ,

$$\begin{aligned}\frac{\partial X}{\partial t} &= -2k_X^2 X^2 + 2k_X^{-2} X_{dim} - k_X^d X - D_X \frac{A}{V} \left( \frac{\partial X}{\partial \theta} \right)_{\theta=L} \\ \frac{\partial X_{dim}}{\partial t} &= k_X^2 X^2 - k_X^{-2} X_{dim} - k_{X_2}^d X_{dim} - D_{X_{dim}} \frac{A}{V} \left( \frac{\partial X_{dim}}{\partial \theta} \right)_{\theta=L}\end{aligned}$$

where  $A$  is the area of the channel cross-section,  $V$  is the compartment volume, and  $X_{dim}$  and  $Y_{dim}$  represent concentrations of the dimeric forms of the proteins  $X$  and  $Y$ .  $P_X$  represents the concentration of free promoter sites on the  $X$  template (i.e. not bound to the  $Y$  dimer), while  $M_X$  represents the concentration of the mRNA transcribed from the  $X$  template.

The above model describing transcription-translation (TX-TL) and dimerisation associated with a single gene regulatory node is used to construct models of all the TX-TL motifs examined in our study (associated parameter values are provided in tables at the end of this document). In particular, the interaction between nodes is always assumed to occur through dimeric regulation (activation or inhibition) by binding to the associated promoter sites, unless otherwise specified.

**Note:** In the case of the two-node activator-inhibitor oscillator we assume self-activation for one of the nodes (the  $X$  node), again through dimeric regulation. In this case, the combined regulation of the  $X$  node by both the  $X$  and  $Y$  dimers is assumed to occur through competitive binding of the two dimers to the  $X$  promoter sites.

We assume  $D_X = D_{X_{dim}}$  and  $k_X^d = k_{X_{dim}}^d$  in all cases in the full computational models (unless otherwise specified). Now, consider the steady state concentration profiles between compartments given by the above model. These must satisfy the equations:

$$\begin{aligned}-2k_X^2 X^2 + 2k_X^{-2} X_{dim} + D_X \frac{\partial^2 X}{\partial \theta^2} &= 0 \\ k_X^2 X^2 - k_X^{-2} X_{dim} + D_{X_{dim}} \frac{\partial^2 X_{dim}}{\partial \theta^2} &= 0\end{aligned}$$

We can now examine different special cases:

(1) No dimerisation involved: if the model does not involve any dimer formation (i.e. we only have the monomeric form), then the steady state concentration profiles of the monomers in the channels satisfy the equation

$$D_X \frac{\partial^2 X}{\partial \theta^2} = 0,$$

and therefore have constant gradients between compartments. This means that, when there is no dimer formation, we can replace the gradient  $\frac{\partial X}{\partial \theta}$  appearing in the transport term for  $X$  by the term  $(\frac{X_2 - X_1}{L})$ , at steady state, in both compartments. This yields a transport term of the form  $p(X_2 - X_1)$  where  $X_1, X_2$  are the concentrations of the  $X$  monomer in two adjacent compartments, and  $p = \frac{DA}{VL}$  is the transport coefficient. This yields a compartmental description of the system that exactly maps onto the PDE at steady state.

(2) With dimerisation, we consider the following special cases:

(a) Equal diffusivities for the monomer and dimer:  $D_X = D_{X_{dim}}$ . This is assumed to be the case in all the numerical simulations and bifurcation analysis of the full PDE models presented in the study. For the concentration profiles in the channel we see that, by multiplying the steady state equation of the dimer (above) by two, and adding this to the steady state equation of the monomer, we have the following equation for the profile of total concentration of protein  $X_T = X + 2X_{dim}$  ([monomer]+2[dimer]):

$$D_X \frac{\partial^2 X_T}{\partial \theta^2} = 0.$$

This implies a constant gradient for  $X_T$  in the channel. Thus, at steady state, we have constant gradients in the channels for the total concentration of protein, while the monomer and dimer concentration profiles generally do not have constant gradients by themselves.

(b) In specific sections below, we make simplifying assumptions for providing analytical insights. Specifically, we assume:

- (i) negligible leak/degradation of dimers in compartments,
- (ii) negligible transport of dimers between compartments,
- (iii) negligible dimerisation in the channel.

These assumptions are used in sections 2 and 3 below. Assumptions (ii) and (iii) imply that at steady state, the protein gradients are constant between the compartments, and this allows us to use a compartmental description for the transport terms - i.e. of the form  $p(X_2 - X_1)$ , where  $X_1, X_2$  are the concentrations of the  $X$  monomer in two adjacent compartments. We will use this description repeatedly in the analysis that follows. We emphasise that these simplifications are employed to obtain transparent analytical insight. Indeed, the full model studied in the text exhibits comparable behaviour even without these simplifications.

## 2 Analysis of non-monotonic variation of steady state concentrations

We have examined the non-monotonic variation of steady state concentrations of the species (proteins) in response to increasing compartment separation, for basic two-node positive and negative regulation. This behaviour, and the underlying trade-offs that cause it, are discussed in the main text.

In all cases, the expressions for the steady state compartmental concentrations ( $X_1, Y_1$  etc.) have been checked by comparison with steady states obtained by numerical solution of the ODE model. The expressions for the derivatives (of steady state compartmental concentrations with respect to the transport coefficient  $p$ ) were calculated using MAPLE 2017. In the following analysis, we assume that the two proteins  $X$  and  $Y$  have equal diffusivity, although the results continue to hold good when this is not the case.

### 2.1 Activation - Monomeric regulation

For the simple activation motif ( $X$  activating  $Y$ ) with  $X$  produced in compartment 1 and the  $Y$  template in compartment 2, we first examine the case with monomeric regulation (no dimerisation). Here,  $p$  is a parameter ( $p = \frac{DA}{VL}$ ) representing the diffusive transport rate between the compartments. Note that  $p$  is positive and inversely proportional to the length  $L$ , of the channel connecting the compartments (i.e. the separation between the compartments in the spatial domain). The steady state equations for the  $X$  and  $Y$

concentrations in the two compartments take the following form:

$$\begin{aligned} k_0 - k_d X_1 - p(X_1 - X_2) &= 0 \\ -k_d X_2 - p(X_2 - X_1) &= 0 \\ -k_d Y_1 - p(Y_1 - Y_2) &= 0 \\ \frac{k_1 X_2}{K + X_2} - k_d Y_2 - p(Y_2 - Y_1) &= 0 \end{aligned}$$

Using these equations, we find

$$\begin{aligned} X_1 &= \frac{k_0 (p + k_d)}{k_d (2p + k_d)}, \quad X_2 = \frac{pk_0}{k_d (2p + k_d)} \\ \frac{dX_1}{dp} &= -\frac{k_0}{(2p + k_d)^2}, \quad \frac{dX_2}{dp} = \frac{k_0}{(2p + k_d)^2} \end{aligned}$$

Thus, increasing channel length/compartment separation leads to an increase in  $X_1$  and a decrease in  $X_2$ .  $X_1$  eventually saturates while  $X_2$  approaches zero. On examining  $Y$ , we have

$$\begin{aligned} Y_2 &= \frac{k_1 p k_0 (p + k_d)}{k_d^2 (2p + k_d)^2} \left( K + \frac{pk_0}{k_d (2p + k_d)} \right)^{-1} \\ \frac{dY_2}{dp} &= \frac{(2Kpk_d^2 + Kk_d^3 - p^2k_0) k_0 k_1}{(2Kpk_d + Kk_d^2 + pk_0)^2 (2p + k_d)^2} \end{aligned}$$

For non-negative values of the parameters, the polynomial in the numerator will always have a single real positive root. Thus,  $Y_2$  can vary non-monotonically with changing compartment separation. Suppose the positive root is at  $p = p^*$ . It is easy to see that the second derivative of  $Y_2$  at  $p^*$  must have the same sign as the derivative of the polynomial at this point ( $\frac{dY_2}{dp}$  has the form  $\frac{f(p)}{g(p)}$  where  $f = 0$  at  $p = p^*$ , and  $g > 0$ ). Thus,  $\frac{d^2 Y_2}{dp^2} = \frac{f'(p^*)}{g(p^*)}$ . Thus,  $Y_2$  has a maximum at  $p^*$ .

Similarly examining  $Y_1$ , we find that

$$\frac{dY_1}{dp} = \frac{(4Kpk_d + 2Kk_d^2 + pk_0) k_0 p k_1}{(2Kpk_d + Kk_d^2 + pk_0)^2 (2p + k_d)^2}$$

Since the polynomial in the numerator can have no positive real roots,  $Y_1$  must vary monotonically for  $p > 0$ .

## 2.2 Activation - Dimeric regulation

For the analysis of this case, it is convenient to use the assumptions discussed in Section 1 - i.e. ignore leak/degradation of the protein dimers, dimerisation in the channel, and transport of the dimers - to obtain the following the steady state equations for the X and Y concentrations:

$$\begin{aligned} k_0 - k_d X_1 - p(X_1 - X_2) &= 0 \\ -k_d X_2 - p(X_2 - X_1) &= 0 \\ -k_d Y_1 - p(Y_1 - Y_2) &= 0 \\ \frac{k_1 X_2^2}{K + X_2^2} - k_d Y_2 - p(Y_2 - Y_1) &= 0 \end{aligned}$$

On examining  $Y_2$ , we have

$$Y_2 = \frac{k_1 p^2 k_0^2 (p + k_d)}{k_d^3 (2p + k_d)^3} \left( K + \frac{p^2 k_0^2}{k_d^2 (2p + k_d)^2} \right)^{-1}$$



$$\frac{dY_2}{dp} = \frac{(4Kp^3k_d^2 + 12Kp^2k_d^3 + 9Kpk_d^4 + 2Kk_d^5 - p^3k_0^2)pk_0^2k_1}{(4Kp^2k_d^2 + 4Kpk_d^3 + Kk_d^4 + p^2k_0^2)^2(2p + k_d)^2}$$

The polynomial in the numerator may be rearranged to give

$$f_2(p) = (4Kk_d^2 - k_0^2)k_0^2k_1p^3 + 12Kk_d^3k_0^2k_1p^2 + 9Kk_d^4k_0^2k_1p + 2Kk_d^5k_0^2k_1$$

Using Descartes' Rule of Signs or otherwise, it can be seen that this polynomial has a single positive real root if  $4Kk_d^2 - k_0^2 < 0$ . As before, we also find that the second derivative of  $Y_2$  at this root is negative. Thus  $Y_2$  can exhibit a maximum if the kinetic parameters satisfy the above condition.

Similarly examining  $Y_1$ , we find that

$$\frac{dY_1}{dp} = \frac{(12Kp^2k_d^2 + 12Kpk_d^3 + 3Kk_d^4 + p^2k_0^2)p^2k_0^2k_1}{(4Kp^2k_d^2 + 4Kpk_d^3 + Kk_d^4 + p^2k_0^2)^2(2p + k_d)^2}$$

Since the polynomial in the numerator can have no positive real roots,  $Y_1$  must vary monotonically for  $p > 0$ . Note that our analysis of the dimeric activation relies on certain simplifying assumptions that do not describe the full system (for which we present computational results in the text). Thus, while this analysis demonstrates the possibility of non-monotonic behaviour shown in the results, it does not guarantee a single maximum, although this is the only behaviour observed computationally.

### 2.3 Repression - Monomeric regulation

Now we examine the simple repression motif (X repressing Y) with X produced in compartment 1 and the Y template in compartment 2. For monomeric regulation, the steady state equations for the X and Y concentrations in the two compartments take the following form:

$$\begin{aligned} k_0 - k_dX_1 - p(X_1 - X_2) &= 0 \\ -k_dX_2 - p(X_2 - X_1) &= 0 \\ -k_dY_1 - p(Y_1 - Y_2) &= 0 \\ \frac{k_1}{K + X_2} - k_dY_2 - p(Y_2 - Y_1) &= 0 \end{aligned}$$

On examining  $Y$ , we have

$$Y_2 = \frac{k_1(p + k_d)}{k_d(2p + k_d)} \left( K + \frac{pk_0}{k_d(2p + k_d)} \right)^{-1}$$

$$\frac{dY_2}{dp} = -\frac{(Kk_d + k_0)k_dk_1}{(2Kpk_d + Kk_d^2 + pk_0)^2}$$

This implies that  $Y_2$  varies monotonically with  $p$ . Similarly examining  $Y_1$ , we find that

$$\frac{dY_1}{dp} = \frac{Kk_d^2k_1}{(2Kpk_d + Kk_d^2 + pk_0)^2}$$

Thus, with monomeric repression,  $Y_1$  varies monotonically with  $p$ , although the trade-off (see main text) is still present.

## 2.4 Repression - Dimeric regulation

With repression of Y by the dimeric form of X, the steady state equations for the X and Y concentrations in the two compartments take the following form:

$$\begin{aligned} k_0 - k_d X_1 - p(X_1 - X_2) &= 0 \\ -k_d X_2 - p(X_2 - X_1) &= 0 \\ -k_d Y_1 - p(Y_1 - Y_2) &= 0 \\ \frac{k_1}{K + X_2^2} - k_d Y_2 - p(Y_2 - Y_1) &= 0 \end{aligned}$$

On examining Y, we have

$$Y_2 = \frac{k_1 (p + k_d)}{k_d (2p + k_d)} \left( K + \frac{p^2 k_0^2}{k_d^2 (2p + k_d)^2} \right)^{-1}$$

$$\frac{dY_2}{dp} = - \frac{(4 K p^2 k_d^2 + 4 K p k_d^3 + K k_d^4 + 3 p^2 k_0^2 + 2 p k_0^2 k_d) k_d^2 k_1}{(4 K p^2 k_d^2 + 4 K p k_d^3 + K k_d^4 + p^2 k_0^2)^2}$$

The numerator polynomial cannot have a real positive root, and therefore  $Y_2$  must vary non-monotonically with  $p$ . Similarly examining  $Y_1$ , we find that

$$\frac{dY_1}{dp} = \frac{(4 K p^2 k_d^2 + 4 K p k_d^3 + K k_d^4 - p^2 k_0^2) k_d^2 k_1}{(4 K p^2 k_d^2 + 4 K p k_d^3 + K k_d^4 + p^2 k_0^2)^2}$$

The numerator polynomial has a single positive real root if  $4 K k_d^2 - k_0^2 < 0$ . We also find that the second derivative of  $Y_1$  at this root is negative. Thus,  $Y_1$  can exhibit a maximum if the kinetic parameters satisfy the above condition.

In conclusion, we see that, as the separation between compartments (channel length) is varied, (i) non-monotonic variation of steady state Y concentration in compartment 2 is possible for the simple activation motif (with either monomeric or dimeric regulation), (ii) non-monotonic variation of steady state Y concentration in compartment 1 is possible for the simple repression motif (with dimeric regulation but not with monomeric regulation).

## 2.5 Mutual-activation motif: effect of spatial separation

In the case of the mutual activation motif distributed between two compartments, varying compartment separation can produce non-monotonic variation of steady state concentrations only in the production compartments. The fact that such behaviour is not possible in the other compartments can be demonstrated as follows, using a compartmental description as above. The steady state equations for the two species X and Y take the following form:

$$\begin{aligned} f_1(Y_1) - k_d X_1 - p(X_1 - X_2) &= 0 \\ -k_d X_2 - p(X_2 - X_1) &= 0 \\ -k_d Y_1 - p(Y_1 - Y_2) &= 0 \\ f_2(X_2) - k_d Y_2 - p(Y_2 - Y_1) &= 0 \end{aligned}$$

where  $f_1$  and  $f_2$  are functions representing activation, and  $p$  is the transport parameter as before. Note that in the case of dimeric regulation, we can make the same approximations as discussed earlier to get these steady state equations. In this case,  $f_1$  and  $f_2$  would be Hill functions of degree 2.

These can be simplified to take the form:

$$\begin{aligned} f_1(Y_1) - g(p)X_1 &= 0 \\ X_2 - h(p)X_1 &= 0 \\ Y_1 - h(p)Y_2 &= 0 \\ f_2(X_2) - g(p)Y_2 &= 0 \end{aligned}$$

where  $g(p) = \frac{k_d^2 + 2k_d p}{k_d + p}$  and  $h(p) = \frac{p}{k_d + p}$ . On differentiating the above with respect to  $p$ , we have the following:

$$\begin{aligned} Y_1' \frac{df_1}{dY_1} - g'X_1 - gX_1' &= 0 \\ X_2' - h'X_1 - hX_1' &= 0 \\ Y_1' - h'Y_2 - hY_2' &= 0 \\ X_2' \frac{df_2}{dX_2} - g'Y_2 - gY_2' &= 0 \end{aligned}$$

The derivatives  $\frac{df_1}{dY_1}$  and  $\frac{df_2}{dX_2}$  are known to be positive. Now, assuming a positive steady state, we consider the possibility that  $X_2$  exhibits non-monotonic behaviour. Thus, for some positive value of  $p$ ,  $X_2' = 0$ . At this point, it can be seen from the last equation that  $Y_2' = -\frac{g'}{g}Y_2$ . Substituting for  $Y_2'$  in the third equation gives  $Y_1' = \frac{gh' - g'h}{g}Y_2$ . For  $p > 0$ , it can be shown that  $gh' - g'h > 0$ . This implies that  $Y_1' > 0$ . Now, setting  $X_2' = 0$  in the second equation gives  $X_1' = -\frac{h'}{h}X_1$ . Substituting for  $X_1'$  in the first equation gives  $Y_1' \frac{df_1}{dY_1} = \frac{g'h - gh'}{h}X_1$ . This implies that  $Y_1' < 0$ . Thus we have a contradiction, and this indicates that non-monotonic behaviour is impossible for  $X_2$ . A similar analysis demonstrates the same for  $Y_1$ .

### 3 Two-node mutual inhibition motif: Simplified model

The results presented in the main text for the mutual inhibition motif involve bifurcation analysis of the distributed circuit. While the one parameter bifurcation diagrams presented were obtained by equilibrium continuation for the full finite-differenced PDE model, for easier computation, we use a simplified description to perform a two parameter analysis. This steady-state compartmental description, is obtained by using the same assumptions discussed previously - ignoring dimerisation in the channel, transport of the dimers, and dimer leak. We note that the qualitative trends seen in the resulting two-parameter bifurcation diagram are reflected in the results of one-parameter analysis of the full spatially discretized model.

With X in compartment 1 and Y in compartment 2 (see main text Figure 3), the model used for the two parameter bifurcation analysis is given by:

$$\begin{aligned} \frac{dX_1}{dt} &= k0_x + \frac{k1_x \alpha P t_x}{1 + K_y Y_1^2} + \frac{k2_x \alpha P t_x K_y Y_1^2}{1 + K_y Y_1^2} - k_d X_1 - p(X_1 - X_2) \\ \frac{dX_2}{dt} &= -k_d X_2 - p(X_2 - X_1) \\ \frac{dY_1}{dt} &= -k_d Y_1 - p(Y_1 - Y_2) \\ \frac{dY_2}{dt} &= \frac{k1_y \alpha P t_y}{1 + K_x X_2^2} + \frac{k2_y \alpha P t_y K_x X_2^2}{1 + K_x X_2^2} - k_d Y_1 - p(Y_2 - Y_1) \end{aligned}$$

As before, we have assumed equal diffusivity for the proteins X and Y - hence the same transport parameter

$p$  appears in all equations. With X and Y co-localised in compartment 1, the model is given by:

$$\begin{aligned}\frac{dX_1}{dt} &= k0_x + \frac{k1_x \alpha P t_x}{1 + K_y Y_1^2} + \frac{k2_x \alpha P t_x K_y Y_1^2}{1 + K_y Y_1^2} - k_d X_1 - p(X_1 - X_2) \\ \frac{dX_2}{dt} &= -k_d X_2 - p(X_2 - X_1) \\ \frac{dY_1}{dt} &= \frac{k1_y \alpha P t_y}{1 + K_x X_1^2} + \frac{k2_y \alpha P t_y K_x X_1^2}{1 + K_x X_1^2} - k_d Y_1 - p(Y_1 - Y_2) \\ \frac{dY_2}{dt} &= -k_d Y_2 - p(Y_2 - Y_1)\end{aligned}$$

In this model, we have three production terms for X, representing (i) expression from a constitutive promoter (this represents an 'input' to the motif (ii) expression from the Y regulated promoter in the unbound state (iii) expression from the same promoter when bound to the Y dimer (transcription factor). For repression, the rate constant of expression for the unbound promoter is much higher than that for the bound promoter ( $k1_x \gg k2_x$ ).

We use bifurcation analysis of the above system to demonstrate the basic role of template concentration and spatial separation in realising bistable behaviour. For this purpose, we fix the ratio of template concentrations of X and Y by fixing  $P t_x$  and  $P t_y$ , and keep this ratio fixed while using  $\alpha$  as a bifurcation parameter. The transport parameter ( $p = \frac{DA}{LV}$ ) is the other bifurcation parameter in this analysis. All other parameters are kept fixed.

The bifurcation analysis of the simplified model is used to obtain the two-parameter plots (see Figure 3) illustrating the interplay between the template concentration and the separation between compartments (channel length). Similar qualitative trends are observed in simulations of the full PDE model, for both the distributed and co-localised configurations.

### 3.1 Modular Augmentation

We also use the above model to examine the possibility of a modular augmentation of the two compartment configuration of this motif (with X and Y apart) by connecting this system to a third compartment (see Fig. S2), assuming equal channel lengths. This new compartment (which we connect to the X compartment here) could represent an 'output' node connected to the existing bistable motif, where we have a template that is regulated in some way by the protein X. Since we focus on the steady state behaviour of the system, we will not introduce this template explicitly. We make the following observations: (i) the behaviour of the motif in the original configuration may be perturbed by the addition of the third compartment, possibly taking it out of the bistable regime (ii) this effect can be mitigated by including a certain amount of X template in the new compartment. In the case examined here, we see that the perturbation introduced by the addition of the new compartment is effectively counteracted by adding a relatively small amount of X template to this compartment (10 percent of the X template present in the original motif).

## 4 Localizing a bistable motif: Well-mixed compartments

While the case of a completely localized bistable circuit in a uniform channel is discussed in the main text, the analogous case for the well-mixed configuration is not. Here we examine this scenario, and see that analogous insights emerge in the context of location dependent behaviour. In order to examine the basic effects of localizing a bistable motif, while letting its output diffuse (and degrade) across the whole domain, we again use the single node, auto-catalytic bistable motif realised using the PEN toolbox (Gines et al. 2017) (Already used in the main text for the analogous case in the uniform channel). This system particularly is suitable for analysis in the present context, as it has only one output species, and involves no dimerisation. In addition, a spatially distributed design (involving localised templates, diffusing output, and uniform degradation) has been realised experimentally (Gines et al. 2017). A simplified ODE model for this motif (as described in Gines et al. (2017)), takes the form:

$$\frac{dx}{dt} = \frac{k_1 x}{K_1 + x} - \frac{k_2 x}{K_2 + x} - k_d x \quad (1)$$

where  $x$  is the concentration of the output species. The first term describes the autocatalytic production of the signal species, the second term describes a saturating degradation pathway for the signal species (realised through a ‘pseudo-template’), while the last term corresponds to a second degradation pathway realised through an exonuclease, that is assumed not to saturate. Before we study the possible spatial organisation of this type of motif, we briefly examine how the degradation rate constant  $k_d$  in the last term, affects bistable behaviour. As seen in Fig. S1(A), increasing  $k_d$  can bring about a saddle node bifurcation that takes the system out of the bistable regime. On the other hand, reducing  $k_d$  cannot take the system out of this regime. This can also be seen analytically, by setting the RHS of (1) to zero, which yields the following cubic equation in  $x$ :

$$-k_d x^3 + (-K_1 k_d - K_2 k_d + k_1 - k_2)x^2 + (-K_1 K_2 k_d - K_1 k_2 + K_2 k_1)x = 0$$

$x = 0$  is one of the roots. For bistability, this polynomial must have two other positive roots. If the remaining parameters are chosen so that the system is bistable for a basal value of  $k_d$ , then it can be demonstrated that there are two positive roots for  $k_d < \frac{k_1 - k_2}{K_1 + K_2}$  and no positive roots otherwise.

Clearly, this condition is violated for large enough  $k_d$ . Thus it is clear that, if we start with a set of parameter values that make the system bistable, then increasing  $k_d$  can make the system monostable. The conclusions that we draw in the following analysis rely on this observation.

#### 4.1 Spatial Separation of the degrading enzyme

Localizing the templates (both the autocatalytic template and the pseudo-template) in one compartment (well-mixed compartment with no leak) and the degrading enzyme in the other (see Fig. S1(B)), creates the possibility of tuning the bistable behaviour of the motif by varying the separation between the compartments. A compartmental description of this system (which is a valid representation at steady state, being equivalent to the PDE) is as follows:

$$\begin{aligned} \frac{k_1 x_1}{K_1 + x_1} - \frac{k_2 x_1}{K_2 + x_1} - p(x_1 - x_2) &= 0 \\ -k_d x_2 - p(x_2 - x_1) &= 0 \end{aligned}$$

This means that the first equation has the form

$$\frac{k_1 x_1}{K_1 + x_1} - \frac{k_2 x_1}{K_2 + x_1} - \tilde{k}_d x_1 = 0$$

where  $\tilde{k}_d = \frac{k_d p}{k_d + p}$ . Thus, the steady state equation for  $x_1$  has the same form as the RHS of (1), with an effective degradation rate constant that is lower than  $k_d$ . This implies two possibilities: (i) If the motif exhibits bistability with co-localised degradation in a single compartment configuration (i.e. the kinetic parameters are such that the basic ODE described above gives bistability), then the motif continues to exhibit bistable behaviour in the distributed configuration (assuming that resource limitations do not come into play); (ii) If the motif is monostable in the co-localised configuration, then it may exhibit bistable behaviour in the distributed configuration, where the effective degradation rate constant is lower. This also indicates the possibility of tuning the switching thresholds of the bistable motif by varying the separation of the templates from the degrading enzyme.

#### 4.2 Placement in a linear array of compartments

If the templates (both the autocatalytic template and the ‘pseudo-template’) are localised in one of a linear array of compartments, each of which has rate constant of leak/degradation associated with it, there is a possibility that the bistable behaviour of the motif may depend on its location within the array. (An equivalent result for the same motif in a uniform 1-D channel is illustrated in the main text (see Figure 6) with the help of bifurcation curves computed through equilibrium continuation for the PDE system.) Here we give an analytical argument that demonstrates the possibility of such behaviour. We will consider a linear configuration of three compartments, with equal leak/degradation rate constants  $\delta$  in each compartment.

The analysis can be extended to any number compartments, with different rate constants of leak, to yield qualitatively similar results.

In the three compartment configuration, there are two possible ways of placing the motif (see Fig. S1(C)): (i) in the middle compartment; (ii) in one of the terminal compartments. Consider case (i). At steady state, a compartmental description of the transport is a valid approximation, and the X concentrations in the three compartments are related by the following equations:

$$\begin{aligned} -\delta x_1 - p(x_1 - x_2) &= 0 \\ \frac{k_1 x_2}{K_1 + x_2} - \frac{k_2 x_2}{K_2 + x_2} - \delta x_2 - p(x_2 - x_1) - p(x_2 - x_3) &= 0 \\ -\delta x_3 - p(x_3 - x_2) &= 0 \end{aligned}$$

This yields the following equation for steady state  $x_2$ , that has the same form as the RHS of (1):

$$\frac{k_1 x_2}{K_1 + x_2} - \frac{k_2 x_2}{K_2 + x_2} - \tilde{k}_d x_2 = 0$$

where the effective degradation rate constant  $\tilde{k}_d = \delta + \frac{2\delta p}{\delta + p}$ . Similarly, in case (ii), the steady state concentrations are related by:

$$\begin{aligned} \frac{k_1 x_1}{K_1 + x_1} - \frac{k_2 x_1}{K_2 + x_1} - \delta x_1 - p(x_1 - x_2) &= 0 \\ -\delta x_2 - p(x_2 - x_1) - p(x_2 - x_3) &= 0 \\ -\delta x_3 - p(x_3 - x_2) &= 0 \end{aligned}$$

This yields the following equation for steady state  $x_1$ , that again has the same form as the RHS of (1):

$$\frac{k_1 x_1}{K_1 + x_1} - \frac{k_2 x_1}{K_2 + x_1} - \hat{k}_d x_1 = 0$$

where the effective degradation rate constant  $\hat{k}_d = \delta + \frac{p\delta(\delta+2p)}{\delta^2+p^2+3\delta p}$ . It can be shown that  $\hat{k}_d < \tilde{k}_d$ . This implies that it is possible that (for certain parameter values) the motif may be bistable in case (ii) and not in case (i). This implies that, even with uniform degradation/leak in all compartments, the location of the motif within a linear array of compartments can determine its behaviour.

### 4.3 Localizing the two node mutual inhibition motif

The basic bistable circuit examined in this study is the two node mutual-inhibition transcription-translation motif. Here we present an analytical argument that allows us to extend the above analysis for the single node bistable motif (realised using the PEN toolbox) to the mutual inhibition motif, under certain conditions. In the analysis above, we have used the ODE model for the bistable motif, and focused on the form of the RHS of (1). Keeping the kinetic parameters fixed, the effect of the spatial organisation is captured by an effective degradation rate constant. We follow the same approach here, and start by examining the ODE model. If dimer leak/degradation is ignored, and we use a quasi-steady state approximation for, the mRNA kinetics, promoter binding and the dimer reactions, the X and Y concentrations satisfy equations of the form:

$$\begin{aligned} \frac{dx}{dt} &= \frac{k_x}{K_x + y^2} - k_d x \\ \frac{dy}{dt} &= \frac{k_y}{K_y + x^2} - k_d y \end{aligned} \tag{2}$$

where we have assumed that the degradation rate/leak is equal for both species. Note that, if X and Y nodes are co-localised in one of the above configurations, at steady state, the  $k_d$  in the above equations is essentially replaced by an 'effective' degradation rate  $k_d^{eff}$ . If X and Y have the same diffusivity,  $k_d^{eff}$  is also the same for both.

Now we examine how the parameter  $k_d$  affects bistability in the system (2). Consider the variable  $u = K_y + x^2$ , for which we have

$$\begin{aligned}\frac{du}{dt} &= 2x \frac{dx}{dt} \\ &= \frac{2xk_x}{K_x + y^2} - 2k_dx^2 \\ &= \frac{2k_x(u - K_y)^{\frac{1}{2}}}{K_x + y^2} - 2k_du + 2k_dK_y\end{aligned}$$

At steady state, we have

$$y = \frac{\gamma}{u} \text{ where } \gamma = \frac{k_y}{k_d}$$

Notice that for non-zero values of  $x$ ,  $\frac{du}{dt} = 0$  implies  $\frac{dx}{dt} = 0$ . Thus, the steady states of the original system correspond to the solutions of the following equation, for  $u > K_y$ :

$$\frac{k_x u^2 (u - K_y)^{\frac{1}{2}}}{K_x u^2 + \gamma^2} - k_d u + k_d K_y = 0$$

Note that  $k_d$  appears in all three of the terms in this equation (in the first term through  $\gamma$ ). We examine the effect of  $k_d$  by plotting two curves for  $u \geq K_y$ :

$$\begin{aligned}f_1(u) &= \frac{k_x u^2 (u - K_y)^{\frac{1}{2}}}{K_x u^2 + \gamma^2} + k_d K_y \\ f_2(u) &= k_d u\end{aligned}$$

The points where the curves intersect (other than  $u = K_y$ ) correspond to the steady states of the system (2). Analysis indicates that we always have  $f_1(u) > f_2(u)$  for  $u$  sufficiently close to  $K_y$ . We also see that, for large  $u$ ,  $f_1(u)$  is  $O(u^{\frac{1}{2}})$ , while  $f_2(u)$  is  $O(u)$ . This means that  $f_1(u) < f_2(u)$  for sufficiently large  $u$ , so that we are guaranteed to have at least one other point of intersection (i.e. steady state). As seen in Fig. S1(D), for kinetic parameters chosen in the bistable regime,  $f_1(u)$  gives a sigmoidal curve that intersects the  $f_2(u)$  curve at three points (other than  $u = K_y$ ). Now we can see what happens when the degradation rate  $k_d$  is increased, keeping the other parameters fixed. As  $k_d$  increases,  $\gamma$  becomes smaller, and this causes the  $f_1(u)$  curve to eventually lose its sigmoidal shape, thus making it impossible to have multiple points of intersection. On the other hand, reducing  $k_d$  preserves the sigmoidal shape of  $f_1(u)$ , and bistability is maintained.

Thus, the effect of the parameter  $k_d$  is essentially similar to that seen in the single node bistable motif realised using the PEN toolbox discussed previously. This means that the insights relating to spatial separation from the degrading enzyme and location dependent bistability in an array of compartments are also applicable to the two node mutual inhibition motif.

## 5 Adaptation to spatial separation

Here we demonstrate the possibility of achieving adaptation of steady state concentration to varying spatial separation between compartments. We do this using simplified models for the kinetics and for simplicity consider the case of monomeric regulation. However, the conclusions do not rely on having monomeric regulation - the results shown in the main text were generated using the full model with dimeric regulation. These results, as well as the following analysis involve having equal diffusivities for X and Y and equal leak/degradation rate constants for both species in a given compartment (While this assumption is sufficient to achieve such adaptive behaviour, we note that it can also be achieved in cases with different diffusivities for X and Y, as long as the leak/degradation rate constants for X and Y in each compartment are in the same ratio as their diffusivities. This condition can be realised when outflow involves a purely diffusive leak

to a zero concentration boundary, as in Karzbrun et al. (2014). In this case, the leak rate constants are essentially proportional to diffusivity, and for different species, will be in the same ratio as the diffusivities.).

We begin our analysis by noting that, in any given network of compartments (with the same structure of transport and leak as used here), there exists a symmetry in how the steady state level in one compartment depends on the production in another. This may be seen as follows. Consider a node X, whose template is localised in a single compartment (compartment  $M$ ) within a network of  $n$  compartments. Using a compartmental model (which is a valid description at steady state), it can be seen that the vector of steady state compartmental concentrations of X in the  $n$  compartments -  $x = [x_1, x_2, \dots, x_n]^T$  (the compartments are numbered from 1 to  $n$ ) - is the solution to a system of linear equations of the form  $Ax = b$ , where the entries of matrix  $A$  are inter-compartmental transport parameters and rate constants of leak from compartments. Since the network of compartments has the structure of an undirected graph, matrix  $A$  is symmetric.

The  $i^{th}$  component of vector  $b$  here is the (zeroth order) production rate of X in compartment  $i$ . In the present scenario, only the  $M^{th}$  component of  $b$  is non-zero -  $b_M = k_x$ , where  $k_x$  is the zeroth order rate constant associated with X production.

Thus, the vector of steady state concentrations is given by  $x_j = A_{j,M}^{-1}b_k = A_{j,M}^{-1}k_x$ . We see that the steady state level in a specific compartment (say compartment  $Q$ ) is given by  $x_Q = A_{Q,M}^{-1}k_x$ . Thus,  $x_Q$  is proportional to the production rate in compartment  $M$ , and the constant of proportionality is  $A_{Q,M}^{-1}$ , which is a function of the degradation rates and the transport parameters. This quantity essentially captures the relationship between production rate in compartment  $M$  and the steady state level in compartment  $Q$ , determined by the structure of the network.

Now let us consider the case where the production is in compartment  $Q$ . The vector of steady states in this case is given by  $x_j = A_{j,Q}^{-1}k_x$ . The level in compartment  $M$  is given by  $x_M = A_{M,Q}^{-1}k_x$ . The constant of proportionality that captures its relationship with the production rate in compartment  $Q$  is thus  $A_{M,Q}^{-1}$ . However, since the matrix  $A$  is symmetric,  $A_{M,Q}^{-1} = A_{Q,M}^{-1}$ . Thus, irrespective of the channel lengths and the leak rate constants in each compartment, the steady state level in compartment M is related to a production in compartment Q in exactly the same way as the steady state level in compartment Q is related to a production in compartment M.

We exploit this symmetry, by combining it with a repressive interaction between two nodes, to allow the steady state level of one of the nodes to adapt in a chosen compartment. The repressive interaction essentially produces the desired cancellation effect needed for adaptation.

## 5.1 Two compartment configuration: X and Y apart

For the two compartment scenario with the X template in the first compartment and its repressor Y being produced in the second compartment, the compartmental concentrations at steady state satisfy the following equations (essentially equivalent to the steady state of the PDE system):

$$\begin{aligned} \frac{k_x}{K_x + y_1} - k_d x_1 - p(x_1 - x_2) &= 0 \\ -k_d x_2 - p(x_2 - x_1) &= 0 \\ -k_d y_1 - p(y_1 - y_2) &= 0 \\ k_y - k_d y_2 - p(y_2 - y_1) &= 0 \end{aligned}$$

where  $p = \frac{DA}{LV}$  is the transport coefficient.

At steady state, the repressor Y concentrations in the compartments are given by,

$$\begin{aligned} y_2 &= \frac{k_y}{H}, \text{ where } H = \frac{k_d^2 + 2k_d p}{k_d + p} \\ y_1 &= G y_2 = \frac{G}{H} k_y, \text{ where } G = \frac{p}{k_d + p} \end{aligned}$$



The X concentrations are:

$$\begin{aligned}
x_1 &= \frac{1}{H} \frac{k_x}{K_x + y_1} \\
x_2 &= Gx_1 = \frac{G}{H} \frac{k_x}{K_x + y_1} \\
&\approx \frac{G}{H} \frac{k_x}{y_1} \quad (\text{in the saturated regime}) \\
&= \frac{k_x}{k_y}
\end{aligned}$$

Note how, as discussed above, the dependence of  $x_2$  on the production rate in compartment 1, and the dependence of  $y_1$  on the production rate in compartment 2 involve the same constant of proportionality:

$$\begin{aligned}
x_2 &= \frac{G}{H} \frac{k_x}{K_x + y_1} = \frac{G}{H} (\text{Production rate of } X \text{ in compartment 1}) \\
y_1 &= \frac{G}{H} k_y = \frac{G}{H} (\text{Production rate of } Y \text{ in compartment 2})
\end{aligned}$$

Thus, we see that the steady state concentration of X in the second compartment (where its repressor Y is produced) is approximately independent of the transport coefficient  $p$ , and therefore of the spatial separation (channel length). This behaviour is also observed computationally, over a range of channel lengths, in the full model (see Figure 2).

## 5.2 Two compartment configuration: X and Y co-localised

For the two compartment scenario with the both X and Y templates in the first compartment and an 'empty' second compartment (potentially containing a template regulated by X or Y), the compartmental concentrations at steady state satisfy the following equations (essentially equivalent to the steady state of the PDE system):

$$\begin{aligned}
\frac{k_x}{K_x + y_1} - k_d x_1 - p(x_1 - x_2) &= 0 \\
-k_d x_2 - p(x_2 - x_1) &= 0 \\
k_y - k_d y_1 - p(y_1 - y_2) &= 0 \\
-k_d y_2 - p(y_2 - y_1) &= 0
\end{aligned}$$

At steady state the repressor Y concentrations in the compartments are given by,

$$\begin{aligned}
y_1 &= \frac{k_y}{H}, \quad \text{where } H = \frac{k_d^2 + 2k_d p}{k_d + p} \\
y_2 &= G y_1 = \frac{G}{H} k_y, \quad \text{where } G = \frac{p}{k_d + p}
\end{aligned}$$

The X concentrations are:

$$\begin{aligned}
x_1 &= \frac{1}{H} \frac{k_x}{K_x + y_1} \\
&\approx \frac{1}{H} \frac{k_x}{y_1} \quad (\text{in the saturated regime}) \\
&= \frac{k_x}{k_y} \\
x_2 &= G x_1 = \frac{G}{H} \frac{k_x}{K_x + y_1}
\end{aligned}$$

Again we note how, as discussed above, the dependence of  $x_1$  on the production rate in compartment 1, and the dependence of  $y_1$  on the production rate in compartment 1 involve the same constant of proportionality:

$$\begin{aligned} x_1 &= \frac{1}{H} \frac{k_x}{K_x + y_1} = \frac{1}{H} (\text{Production rate of } X \text{ in compartment 1}) \\ y_1 &= \frac{1}{H} k_y = \frac{1}{H} (\text{Production rate of } Y \text{ in compartment 1}) \end{aligned}$$

Thus, we see that the steady state concentration of X in the first compartment (where both X and its repressor Y are produced) is approximately independent of the transport coefficient  $p$ , and therefore of the spatial separation (channel length). This behaviour is also observed computationally, over a range of channel lengths, in the full model (see Figure 2).

### 5.3 Effect of additional upstream regulation of X

Here we have considered a case where the expression of X is regulated only by the node Y. However, we note that the both the above result and the subsequent ones below, are also valid when X is subject to additional regulation by another input (say Z) produced in a different compartment, as long as this regulation does not involve competition for binding sites with the repressor Y, and does not interfere with the Y regulation in any other way. Under such conditions, the basal production rate of X,  $k_x$  becomes  $k_x(z)$ , i.e. a function of the input Z, while the rest of the model remains the same. The level of Z in the X compartment would, of course, also have to be maintained in order for X to adapt as desired. If we require X to adapt in a different compartment to where it is produced, this can be achieved by the same approach, having a different repressor (i.e. distinct from Y) for Z, that is produced in the X compartment. If we require X to adapt in its production compartment, then the repressor node Y is co-localised with X, and we only need Y to also repress Z, in order to maintain level of Z in the X compartment.

**Note:** Note that negative autoregulation (i.e. repression of X transcription by the X protein) does not produce the type of adaptive behaviour described above.

We now examine a three compartment configuration to demonstrate that this approach to achieving adaptation to varying spatial separation (channel lengths) is also applicable to configurations involving more compartments.

### 5.4 Three compartments: Case 1

For the three compartment scenario with the X template in the first compartment, its repressor Y being produced in the second compartment, and a third compartment potentially containing a template that is regulated by X and/or Y. Since the presence/absence of a template in the third compartment does not affect the steady state concentrations of X or Y in any of the compartments, and only contributes through the leak of X and Y from this compartment, we will treat this compartment as empty for the purposes of this analysis. The compartmental concentrations at steady state satisfy the following equations (essentially equivalent to the steady state of the PDE system):

$$\begin{aligned} \frac{k_x}{K_x + y_1} - k_d x_1 - p_1(x_1 - x_2) &= 0 \\ -k_d x_2 - p_1(x_2 - x_1) - p_2(x_2 - x_3) &= 0 \\ -k_d x_3 - p_2(x_3 - x_2) &= 0 \\ -k_d y_1 - p_1(y_1 - y_2) &= 0 \\ k_y - k_d y_2 - p_1(y_2 - y_1) - p_2(y_2 - y_3) &= 0 \\ -k_d y_3 - p_2(y_3 - y_2) &= 0 \end{aligned}$$

At steady state the repressor Y concentrations in the compartments are given by,

$$\begin{aligned} y_1 &= G_1 y_2, \text{ where } G_1 = \frac{p_1}{k_d + p_1} \\ y_3 &= G_2 y_2, \text{ where } G_2 = \frac{p_2}{k_d + p_2} \\ y_2 &= \frac{k_y}{F}, \text{ where } F = k_d + p_1(1 - G_1) + p_2(1 - G_2) \end{aligned}$$

The X concentrations are:

$$\begin{aligned} x_3 &= G_2 x_2 \\ x_2 &= H x_1, \text{ where } H = \frac{p_1}{k_d + p_1 + \frac{p_2 k_d}{k_d + p_2}} \\ x_1 &= \frac{1}{k_d + p_1(1 - H)} \frac{k_x}{K_x + y_1} \end{aligned}$$

Thus, in a regime where  $y_1$  is saturating, we have

$$\begin{aligned} x_1 &\approx \frac{1}{k_d + p_1(1 - H)} \frac{k_x}{y_1} \\ &= \frac{1}{k_d + p_1(1 - H)} \frac{k_x}{G_1 y_2} \end{aligned}$$

It can be shown that:

$$\frac{G_1}{F} = \frac{H}{(k_d + p_1(1 - H))}$$

Note how this implies that:

$$\begin{aligned} x_2 &= \frac{G_1}{F} \frac{k_x}{K_x + y_1} = \frac{G_1}{F} (\text{Production rate of } X \text{ in compartment 1}) \\ y_1 &= \frac{G_1}{F} k_y = \frac{G_1}{F} (\text{Production rate of } Y \text{ in compartment 2}) \end{aligned}$$

again reflecting how the dependence of  $x_2$  on the production rate in compartment 1, and the dependence of  $y_1$  on the production rate in compartment 2 involve the same constant of proportionality.

Thus, in the saturation regime,  $x_2$  and  $x_3$  are given by:

$$\begin{aligned} x_2 &= H x_1 \approx \frac{H}{k_d + p_1(1 - H)} \frac{k_x F}{G_1 k_y} = \frac{k_x}{k_y} \\ x_3 &= G_2 x_2 \approx \frac{k_x p_2}{k_y (k_d + p_2)} \end{aligned}$$

Thus, we see that  $x_2$  adapts to changes in  $p_1$  or  $p_2$  (i.e. varying the length of either channel), while  $x_3$  adapts only to changes in  $p_1$ .

## 5.5 Three compartments: Case 2

Now we examine the case where X and Y are in the terminal compartments of a three compartment configuration, with the middle compartment treated as empty (as we have done above). The compartmental concentrations at steady state satisfy the following equations (essentially equivalent to the steady state of the PDE system):

$$\begin{aligned}
\frac{k_x}{K_x + y_1} - k_d x_1 - p_1(x_1 - x_2) &= 0 \\
-k_d x_2 - p_1(x_2 - x_1) - p_2(x_2 - x_3) &= 0 \\
-k_d x_3 - p_2(x_3 - x_2) &= 0 \\
-k_d y_1 - p_1(y_1 - y_2) &= 0 \\
-k_d y_2 - p_1(y_2 - y_1) - p_2(y_2 - y_3) &= 0 \\
k_y - k_d y_3 - p_2(y_3 - y_2) &= 0
\end{aligned}$$

At steady state the repressor Y concentrations in the compartments are given by,

$$\begin{aligned}
y_2 &= H_y y_3, \text{ where } H_y = \frac{p_2}{k_d + p_2 + \frac{p_1 k_d}{k_d + p_1}} \\
y_1 &= G_y y_2, \text{ where } G_y = \frac{p_1}{k_d + p_1} \\
y_3 &= \frac{k_y}{k_d + p_2(1 - H_y)}
\end{aligned}$$

The X concentrations are:

$$\begin{aligned}
x_2 &= H_x x_1, \text{ where } H_x = \frac{p_1}{k_d + p_1 + \frac{p_2 k_d}{k_d + p_2}} \\
x_3 &= G_x x_2, \text{ where } G_x = \frac{p_2}{k_d + p_2} \\
x_1 &= \frac{k_x}{K_x + y_1} \left( \frac{1}{k_d + p_1(1 - H_x)} \right)
\end{aligned}$$

It can be shown that:

$$\begin{aligned}
\frac{G_y H_y}{(k_d + p_2(1 - H_y))} &= \frac{G_x H_x}{(k_d + p_1(1 - H_x))} \\
&= \frac{G_x G_y}{k_d(1 + G_x + G_y)}
\end{aligned}$$

Note how this implies that:

$$\begin{aligned}
x_3 &= \frac{G_x G_y}{k_d(1 + G_x + G_y)} \frac{k_x}{K_x + y_1} = \frac{G_x G_y}{k_d(1 + G_x + G_y)} (\text{Production rate of X in compartment 1}) \\
y_1 &= \frac{G_x G_y}{k_d(1 + G_x + G_y)} k_y = \frac{G_x G_y}{k_d(1 + G_x + G_y)} (\text{Production rate of Y in compartment 3})
\end{aligned}$$

again reflecting how the dependence of  $x_3$  on the production rate in compartment 1, and the dependence of  $y_1$  on the production rate in compartment 3 involve the same constant of proportionality.

Thus, in a regime where  $y_1$  is saturating, we have

$$\begin{aligned}
x_1 &\approx \frac{1}{k_d + p_1(1 - H_x)} \frac{k_x}{y_1} \\
&= \frac{1}{k_d + p_1(1 - H_x)} \frac{k_x}{G_y H_y y_3}
\end{aligned}$$

This means that  $x_3$  is given by:

$$\begin{aligned} x_3 = G_x H_x x_1 &\approx \left( \frac{k_x}{k_y} \right) \left( \frac{G_x H_x}{G_y H_y} \right) \left( \frac{k_d + p_2(1 - H_y)}{k_d + p_1(1 - H_x)} \right) \\ &= \frac{k_x}{k_y} \end{aligned}$$

Thus, the concentration of X in the third compartment (where Y is produced) is essentially independent of both the transport coefficients (and therefore also independent of the channel lengths). Also note that  $x_2 = \frac{x_3}{G_x}$ , and therefore  $x_2$  is independent of the transport coefficient  $p_1$ .

**Note:** While the steady state level only in the repressor compartment adapts to changes in the lengths of all the channels in the network, the level in other compartments can also adapt to changes in the lengths of certain channels - i.e. those not contained in any paths connecting these compartments to the repressor compartment. This is because the steady state levels in these compartments are essentially proportional to the level in the repressor compartment, with the associated constants of proportionality only involving only those transport parameters associated with the paths connecting these compartments to the repressor compartment.

## 5.6 General case

The above results, for the two and three compartment configurations, can also be demonstrated through a more general approach involving an arbitrary network of compartments. Consider a node X, whose template is localised in multiple compartments within such a network. Using a compartmental model (as above), it can be seen that the vector of steady state compartmental concentrations of X -  $x = [x_1, x_2, \dots, x_n]^T$  (the compartments are numbered from 1 to  $n$ ) - is the solution to a system of linear equations of the form  $A_X x = b_X$ . The  $i^{th}$  component of vector  $b_X$  here is the (zeroth order) production rate of X in compartment  $i$ . The matrix  $A_X$  is symmetric (since the network of compartments has the structure of an undirected graph), and its entries are inter-compartmental transport parameters and rate constants of leak from compartments. Now suppose the repressor Y is produced in compartment  $j$  (only in this compartment). The steady state levels of Y also satisfies a system of linear equations  $A_Y y = b_Y$ .

We note the following points: (i) if X and Y have essentially the same diffusivity (hence also the same transport parameters and rate constants of leak in each compartment), then the matrices  $A_X$  and  $A_Y$  are identical - we call it  $A$  (ii) the vector  $y$  of steady state concentrations is given by  $y_i = k_y A_{i,j}^{-1}$  where  $k_y$  is the production rate of Y in compartment  $j$  (It is zero elsewhere). (iii) If the production rate of X in the  $i^{th}$  compartment is given by  $\frac{k_i^X}{K_X + y_i}$ , then in a saturated regime (substituting for the  $y_i$  from the previous step), the vector  $b_X$  is approximately given by  $b_X = [\frac{k_1^X}{k_y A_{1,j}^{-1}}, \frac{k_2^X}{k_y A_{2,j}^{-1}}, \dots, \frac{k_n^X}{k_y A_{n,j}^{-1}}]^T$ . (iv) The level of X in compartment  $j$  (where Y is produced) is therefore given by  $x_j = \sum_i \frac{k_i^X A_{j,i}^{-1}}{k_y A_{i,j}^{-1}}$ . Since the matrix  $A$  is symmetric, so is its inverse, and therefore we have  $x_j = \frac{1}{k_y} \sum_i k_i^X$ .

The above result suggests the following interpretations: (i)  $x_j$  adapts to changing the connectivity between compartments, as long as none of the X producing compartments becomes disconnected (ii)  $x_j$  adapts to the addition of a new compartment, as long as this does not introduce additional X production (iii)  $x_j$  adapts to changes in the separation between compartments (assuming that the resulting change in transport parameters is the same for X and Y) (iv)  $x_j$  adapts to changing the location  $j$  of repressor production

We note that the above results are valid only if the assumption of saturation in the regulation by the repressor continues to hold good. From the above analysis, it can also be seen how the adaptive behaviour can be achieved with different diffusivities for X and Y. If the leak rate constants for X and Y in each compartment are in the same ratio as their diffusivities (the inter-compartmental transport parameters are, of course, proportional to the diffusivities - see Section 1), it can be seen that, while the matrices  $A_X$  and  $A_Y$  are not identical, one is a scalar multiple of the other, i.e.  $A_Y = \frac{D_Y}{D_X} A_X$ . As a result, the cancellation effect (seen above) that produces the adaptive behaviour is maintained (the only difference being the appearance of an additional factor in the expression for  $x_j$ , i.e. the ratio of diffusivities)

## 5.7 Dimeric regulation

The analysis above is confined to the case of monomeric regulation by the repressor, with no dimer formation involved for X or Y. However, computational results for analogous circuits with dimerisation (presented in the main text - see Fig. 2) show that these circuits are also capable of the same qualitative behaviour - i.e. adaptation of the steady state compartmental monomer and dimer concentrations in the compartment containing repressor production. Here we explain why this occurs, by examining the two compartment scenario with X and Y apart (analogous to the scenario in Section 5.1).

We begin by noting the following points relating the dimeric case: (i) In the dimeric case, if we assume equal diffusivities and equal leak rate constants for monomers and dimers, the total protein concentrations in the compartments at steady state ( $x_1^T = x_1 + 2x_{dim1}$ ) satisfy equations of exactly the same form as the steady state monomer concentrations in the monomeric case - i.e. equations of the same form as those in Section 5.1. Since the total concentration of protein also has constant gradient in the channel at steady state (see Section 1), the compartmental description for the total concentrations (with transport coefficient  $p = \frac{DA}{LV}$ ) is essentially equivalent to the PDE at steady state. We explicitly demonstrate this equivalence for the compartmental concentrations below.

For Y, the compartmental steady state concentrations satisfy:

$$-k_d y_1 - p(y_1 - y_2) - 2k_Y^{dim} y_1^2 + 2k_Y^{diss} y_{dim1} = 0 \quad (3)$$

$$-k_d y_{dim1} - p(y_{dim1} - y_{dim2}) + k_Y^{dim} y_1^2 - 2k_Y^{diss} y_{dim1} = 0 \quad (4)$$

$$k_y - k_d y_2 - p(y_2 - y_1) 2k_Y^{dim} y_2^2 + 2k_Y^{diss} y_{dim2} = 0 \quad (5)$$

$$-k_d y_{dim2} - p(y_{dim2} - y_{dim1}) + k_Y^{dim} y_2^2 - 2k_Y^{diss} y_{dim2} = 0 \quad (6)$$

Adding equations (3)+(4) and equations (5)+(6) gives us the following equations for the total concentration of protein  $y_1^T = y_1 + 2y_{dim1}$  and  $y_2^T = y_2 + 2y_{dim2}$ :

$$\begin{aligned} -k_d y_1^T - p(y_1^T - y_2^T) &= 0 \\ k_y - k_d y_2^T - p(y_2^T - y_1^T) &= 0 \end{aligned}$$

Note how these equations have exactly the same form as those in Section 5.1. A similar analysis applies for the protein X, giving us (as before) the following dependence for  $y_1^T$  on the Y production in compartment 2 and for  $x_2^T$  on the X production in compartment 1:

$$\begin{aligned} y_1^T &= \frac{G}{H} k_y = \frac{G}{H} (\text{Production rate of Y in compartment 2}) \\ x_2^T &= \frac{G}{H} \frac{k_x}{K_x + y_{dim1}} = \frac{G}{H} (\text{Production rate of X in compartment 1}) \end{aligned}$$

where  $G$  and  $H$  are exactly as given in Section 5.1.

(ii) Now, among the parameter values used, the dimerisation and dimer dissociation rate constants are at least an order of magnitude higher than the other rate constants (both reaction rate constants and effective rate constants of transport). This means that, there is a quasi-equilibrium between the monomer and the dimer concentrations in the compartments (confirmed by computational results for the full model)

(iii) If, in addition, the dimerisation and dimer dissociation rate constants for Y are of comparable magnitude, or the dimerisation rate constant is significantly higher, the total protein concentration at steady state is dominated by the dimer contribution - i.e.  $y_1^T \approx 2y_{dim1}$ , and  $y_2^T \approx 2y_{dim2}$ . This fact is also confirmed by computational results for the full model.

The insight revealed in (iii) can be combined with (i) to see that (in the saturation limit)  $x_2^T$  is approximately given by:

$$x_2^T = \frac{G}{H} \frac{k_x}{K_x + y_{dim1}} \approx \frac{G}{H} \frac{k_x}{y_{dim1}} \approx \frac{G}{H} \frac{k_x}{\frac{y_1^T}{2}} = \frac{2k_x}{k_y}$$

Thus, we see that the total concentration of protein X in compartment 2 is essentially independent of the transport coefficient, exactly as seen for the monomer concentration in section 5.1. Furthermore, from point (ii) it follows that in this case, the monomer and dimer concentrations of X in compartment 2 taken individually, would also be independent of the transport coefficient. Note that dimerisation of X is not necessary for this result to hold.

The above analysis demonstrates that in a certain parameter regime - i.e. with the dimerisation and dimer dissociation rate constants significantly higher than the other rate constants, and with the dimer form essentially dominating the total concentration for the repressor, our analysis and the resulting insights for the purely monomeric case (presented earlier) are directly applicable to the case of dimeric regulation. In fact, similar considerations indicate that these are also relevant to regulation by higher multimeric forms. Also note that no additional assumptions about dimer transport, dimer leak, or dimerisation in the channel were needed in the above analysis.

## 5.8 Adaptation to template concentrations

The circuits implemented in Bleris et al. (2011), for adaptation to template concentration, are based on incoherent feedforward regulation of the output, at either the transcriptional or the post-transcriptional level, by a second species produced from the same template. In either case, under certain assumptions, the steady state relationship between the input  $x$  (concentration of template) and the output  $y$  (protein concentration) takes the form:

$$y = \frac{Vx}{K + x}$$

Now, in the context of the present discussion (see above), it is easy to see that the same type of circuit (i.e. with X and Y produced from the same template) could also exhibit adaptation to spatial separation, as seen for the case where X and Y are co-localised (section 5.2). In this case, assuming monomeric regulation of X by Y, the steady-state compartmental concentrations satisfy the following equations reads

$$\begin{aligned} \frac{k_x S}{K_x + y_1} - k_d x_1 - p(x_1 - x_2) &= 0 \\ -k_d x_2 - p(x_2 - x_1) &= 0 \\ k_y S - k_d y_1 - p(y_1 - y_2) &= 0 \\ -k_d y_2 - p(y_2 - y_1) &= 0 \end{aligned}$$

where  $S$  represents the template concentration. As before, the steady-state value of  $x_1$  is given by:

$$\begin{aligned} x_1 &= \frac{1}{H} \frac{k_x S}{K_x + y_1} \\ &\approx \frac{1}{H} \frac{k_x S}{\left(\frac{k_y S}{H}\right)} \quad (\text{in the saturated regime}) \\ &= \frac{k_x}{k_y} \end{aligned}$$

This essentially means that the steady state concentration of X, in the compartment where it is produced, adapts to both variation in channel lengths, and variation in the template concentration.

If we now want to achieve this type of combined adaptation of X to both spatial separation and X template concentration in a different compartment (i.e. not where the X template is located), then we find that this requires a combined regulation of X production by two repressors (say Y and Z). A possible circuit design that achieves this is as follows: one repressor (Y) is produced from the same template as X, while the other (Z) is produced in the compartment where we require adaptation of X. Here we examine such a circuit, with monomeric regulation, in a two compartment configuration, with X and Y produced (from the same template) in compartment 1 and Z produced in compartment 2. We first examine the case where Z only represses X, and does not regulate Y. If we assume equal diffusivities, and that the combined regulation of X by Y and Z does not involve competition for binding sites, we have the following equations for the steady state concentrations:

$$\begin{aligned}
\frac{k_x S}{(K_{xy} + y_1)(K_{xz} + z_1)} - k_d x_1 - p(x_1 - x_2) &= 0 \\
-k_d x_2 - p(x_2 - x_1) &= 0 \\
k_y S - k_d y_1 - p(y_1 - y_2) &= 0 \\
-k_d y_2 - p(y_2 - y_1) &= 0 \\
-k_d z_1 - p(z_1 - z_2) &= 0 \\
k_z - k_d z_2 - p(z_2 - z_1) &= 0
\end{aligned}$$

Solving for the steady state as before, we have

$$\begin{aligned}
z_2 &= \frac{k_y}{H}, \text{ where } H = \frac{k_d^2 + 2k_d p}{k_d + p} \\
z_1 &= G y_2 = \frac{G}{H} k_z, \text{ where } G = \frac{p}{k_d + p} \\
y_1 &= \frac{k_y S}{H} \\
y_2 &= \frac{G}{H} k_y S
\end{aligned}$$

This means that, for X, we have

$$\begin{aligned}
x_1 &= \frac{1}{H} \frac{k_x S}{(K_{xy} + y_1)(K_{xz} + z_1)} \\
&\approx \frac{1}{H} \frac{k_x S}{\left(\frac{k_y S}{H}\right) \left(\frac{G k_z}{H}\right)} \text{ (in the saturated regime)} \\
&= \frac{k_x}{k_y k_z} \left(\frac{H}{G}\right) \\
x_2 &= G x_1 \approx \frac{k_x}{k_y k_z} H
\end{aligned}$$

This means that, although  $x_2$  is approximately independent of the template concentration S, it still depends on the transport coefficient, and therefore does not adapt to changing compartment separation. However, if Y is essentially non-diffusible, we have  $y_1 = \frac{k_y S}{k_d}$ , in which case, we have  $x_1 \approx \frac{k_x}{k_y k_z} \left(\frac{k_d}{G}\right)$  and  $x_2 \approx \frac{k_x}{k_y k_z} k_d$ . Thus, if Y does not diffuse,  $x_2$  is approximately independent of both the template concentration and the compartment separation, and we get the desired behaviour.

If we now examine the case where both X and Y production is repressed by Z, a similar analysis (again in the saturated regime) shows that while  $x_2$  approximately adapts to the template concentration, it continues to depend on the transport coefficient, regardless of whether Y is diffusible or not.

To summarise, for the case of monomeric regulation, we need Y and Z to meet the following conditions: (i) while Z represses X production, it must not repress Y production, (ii) the combined regulation of X

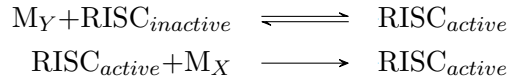


by Y and Z should not involve competition for binding sites, (iii) Y must be essentially confined to the compartment where it is produced. A circuit that satisfies these constraints will allow the steady state concentration of X in the Z compartment to adapt to both variation in compartment spacing and variation in template concentration.

## 5.9 Exemplar case: combined adaptation to template concentration and spatial separation

We present computational results in the main text, showing how adaptation to both of the above factors can be achieved by one possible realisation of such a circuit. The particular realisation considered here involves having one of the repressor nodes (Y) act at the translational level - with the mRNA from node Y activating an RNA induced silencing complex (RISC)- and the other (Z) acting at the transcriptional level - the protein from node Z acting as a transcription factor. While the protein from node Z inhibits transcription of node X (through dimeric regulation), the RISC activated by mRNA expressed constitutively from node Y degrades the mRNA produced by transcription at node X. Having the two repressing nodes act at different steps precludes any competitive effects in their regulation of X. In addition, having the mRNA from the Y node act as the regulator allows its effect to be essentially confined to its production compartment, since the mRNA diffusion is assumed to be slow relative to its degradation.

For the exemplar case shown in the text, in addition to all the basic ingredients of our model, we assume a fixed total concentration (active and inactive forms) of the silencing complex in the compartment where the template for X (and Y) is placed. In addition to the basic transcription/translation reactions, the following reactions involving the RISC are assumed to take place in this compartment (following the simplified model used in Bleris et al. (2011)):



where  $M_Y$  and  $M_X$  denote the mRNA transcript associated with nodes Y and X. The kinetics of these mRNA transcripts and the RISC (in the compartment containing the X-Y template) is modelled using mass action kinetics (similar to Bleris et al. (2011)):

$$\begin{aligned} \frac{dM_Y}{dt} &= r_Y^c P_X^T - r_X^d M_Y - k_b M_Y [\text{RISC}_{inactive}] + k_u [\text{RISC}_{active}] \\ \frac{d[\text{RISC}_{active}]}{dt} &= k_b M_Y [\text{RISC}_{inactive}] - k_u [\text{RISC}_{active}] \\ \frac{dM_X}{dt} &= r_X^c (P_X^T - P_X) + r_X^z P_X - r_X^d M_X - r_X^{\text{RISC}} [\text{RISC}_{active}] M_X \end{aligned}$$

with the conservation condition

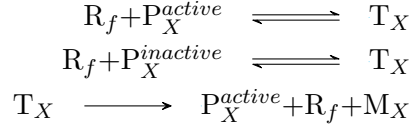
$$[\text{RISC}_{total}] = [\text{RISC}_{inactive}] + [\text{RISC}_{active}]$$

For the computational results shown, the  $[\text{RISC}_{total}]$  is taken to be high so that saturation of the RISC does not come into play.

## 6 Effect of competition for resources - Fixed total RNAP

The effect of resource competition between different nodes in a genetic activation cascade, including competition for RNAPs and ribosomes, have been examined in detail by Qian et al. (2017). Here we demonstrate both the possible use of compartmentalisation (that decouples the resources) to mitigate these effects, and a resulting trade-off that may result in lower output levels. For simplicity, we focus on a single resource -

the RNAP enzyme, for which fix the total concentration (free + bound to template). Other resources are assumed to be non-limiting. We consider a three node activation cascade where X activates Y and X itself is activated by an input I. We consider the following reactions involving the RNAP:



where  $R_f$  is the free RNAP,  $P_X^{active}$  is the promoter activator complex (i.e. bound to the input transcription factor),  $P_X^{inactive}$  is the inactive form of the promoter,  $T_X$  is the transcription complex, and  $M_X$  is the mRNA transcript for X. The rate constants, for binding and unbinding of the free RNAP to form the transcription complex, are chosen to reflect the high binding affinity of the active form relative to the inactive form. We consider the same reactions for the RNAP at the Y node. The total concentration of RNAP, which we keep fixed, is therefore given by

$$[R]_{total} = [R_f] + [T_X] + [T_Y]$$

The basic effect, which is essentially a biphasic response of the output Y to increasing concentration of input I, results from the fact that the nodes X and Y (with transcription factor bound to the promoter) compete for the RNAP. We note that, in the context of co-localised nodes in a spatially distributed configuration (for instance the well-mixed compartments), this type of effect could potentially combine with the basic trade-offs that give rise to non-monotonic behaviour (Section 2).

As discussed in the main text, spatial separation that decouples the resources used by the two nodes is one possible way of mitigating this type of competition effect. However, a trade-off arises in this case due to potential signal attenuation between nodes, depending on the compartment separation and the leaks. This is illustrated in the main text (Figure 5) using computational results obtained for the full model.

## 7 Single production compartment in a uniform channel

### 7.1 Open boundaries and no degradation

For a single node, with constant production of signal species, localised over  $\theta \in [\theta_1, \theta_2]$  in a 1-D domain of  $L = 1$  with no degradation, the simplified model is as follows: For  $\theta \in [0, \theta_1)$ ,

$$\frac{\partial[X]}{\partial t} = D_X \frac{\partial^2[X]}{\partial \theta^2}$$

For  $\theta \in [\theta_1, \theta_2]$ ,

$$\frac{\partial[X]}{\partial t} = k_0 + D_X \frac{\partial^2[X]}{\partial \theta^2}$$

For  $\theta \in [\theta_2, 1)$ ,

$$\frac{\partial[X]}{\partial t} = D_X \frac{\partial^2[X]}{\partial \theta^2}$$

With homogeneous Dirichlet boundaries, the solution is given by:

For  $\theta \in [0, \theta_1)$ ,

$$X = \frac{k_0}{D} \theta (\theta_2 - \theta_1) \left(1 - \frac{\theta_1 + \theta_2}{2}\right) \quad (7)$$

For  $\theta \in [\theta_1, \theta_2]$ ,

$$X = \frac{k_0}{D} \theta (\theta_2 - \theta) \left(1 - \frac{\theta + \theta_2}{2}\right) + \frac{k_0}{2D} (1 - \theta) (\theta^2 - \theta_1^2) \quad (8)$$

For  $\theta \in [\theta_2, 1)$ ,

$$X = \frac{k_0}{2D}(1 - \theta)(\theta_2^2 - \theta_1^2) \quad (9)$$

Using the above solution, we note the following: Suppose we have constant production (rate  $k_0$ ) localised in a compartment (compartment 1) of size  $l$  centred at location  $p_1$  in the domain. Consider as second (empty) compartment (compartment 2) of the same size, centred at location  $p_2$  ( $p_2 > p_1$ ), such that the two compartments do not overlap. Using (9) above, and averaging over compartment 2, we see that the average concentration of  $X$  over this compartment is given by:

$$\langle X \rangle_2 = \frac{k_0 l}{D}(1 - p_2)p_1 = \frac{l(1 - p_2)p_1}{D}(\text{Production rate of } X \text{ in compartment 1}) \quad (10)$$

Now consider the case where the production is in compartment 2. Here we use (7) above to calculate the average:

$$\langle X \rangle_1 = \frac{k_0 l}{D}p_1(1 - p_2) = \frac{lp_1(1 - p_2)}{D}(\text{Production rate of } X \text{ in compartment 2}) \quad (11)$$

From (10) and (11) above, it is clear that the constant of proportionality multiplying the production rate is the same in both cases. Thus we find that, analogous to the case of well-mixed compartments (see Section 5), the steady state level in compartment 1 is related to a production in compartment 2 in exactly the same way as the steady state level in compartment 2 is related to a production in compartment 1.

## 7.2 Closed boundaries and uniform degradation

For a single node, with constant production of signal species, localised over  $\theta \in [\theta_1, \theta_2]$  in a 1-D domain of  $L = 1$  with uniform degradation, the simplified model is as follows:

For  $\theta \in [0, \theta_1)$ ,

$$\frac{\partial[X]}{\partial t} = -k_d X + D_X \frac{\partial^2[X]}{\partial \theta^2}$$

For  $\theta \in [\theta_1, \theta_2]$ ,

$$\frac{\partial[X]}{\partial t} = k_0 - k_d X + D_X \frac{\partial^2[X]}{\partial \theta^2}$$

For  $\theta \in [\theta_2, 1)$ ,

$$\frac{\partial[X]}{\partial t} = -k_d X + D_X \frac{\partial^2[X]}{\partial \theta^2}$$

With homogeneous Neumann boundaries, the solution is given by:

For  $\theta \in [0, \theta_1)$ ,

$$X = \frac{k_0 \cosh(\omega \theta)}{k_d \sinh(\omega)} (\sinh(\omega(1 - \theta_1)) - \sinh(\omega(1 - \theta_2))) \quad (12)$$

For  $\theta \in [\theta_1, \theta_2]$ ,

$$\begin{aligned} X = & \frac{k_0 \cosh(\omega \theta)}{k_d \sinh(\omega)} (\sinh(\omega(1 - \theta)) - \sinh(\omega(1 - \theta_2))) \\ & + \frac{k_0 \cosh(\omega(1 - \theta))}{k_d \sinh(\omega)} (\sinh(\omega \theta) - \sinh(\omega \theta_1)) \end{aligned} \quad (13)$$

For  $\theta \in [\theta_2, 1)$ ,

$$X = \frac{k_0 \cosh(\omega(1 - \theta))}{k_d \sinh(\omega)} (\sinh(\omega \theta_2) - \sinh(\omega \theta_1)) \quad (14)$$

where  $\omega = \sqrt{\frac{k_d}{D}}$ .

If we now consider two compartments as before, with constant production localised in one of them, the above solution can be used to once again see that the steady state level in compartment 1 (centred at  $p_1$ ) is related to a production in compartment 2 (centred at  $p_2$  ( $p_1 < p_2$ )) in exactly the same way as the steady state level in compartment 2 is related to a production in compartment 1.

Using (14) above, we find:

$$\begin{aligned}\langle X \rangle_2 &= \frac{4 \sinh^2(\frac{\omega l}{2}) k_0}{l k_d \omega \sinh(\omega)} \cosh(\omega p_1) \cosh(\omega(1 - p_2)) \\ &= \frac{4 \sinh^2(\frac{\omega l}{2})}{l k_d \omega \sinh(\omega)} \cosh(\omega p_1) \cosh(\omega(1 - p_2)) (\text{Production rate of } X \text{ in compartment 1})\end{aligned}\quad (15)$$

Now consider the case where the production is in compartment 2. Here we use (12) above to calculate the average:

$$\begin{aligned}\langle X \rangle_1 &= \frac{4 \sinh^2(\frac{\omega l}{2}) k_0}{l k_d \omega \sinh(\omega)} \cosh(\omega(1 - p_2)) \cosh(\omega p_1) \\ &= \frac{4 \sinh^2(\frac{\omega l}{2})}{l k_d \omega \sinh(\omega)} \cosh(\omega(1 - p_2)) \cosh(\omega p_1) (\text{Production rate of } X \text{ in compartment 2})\end{aligned}\quad (16)$$

From (15) and (16), it is clear that the constant of proportionality multiplying the production rate is the same in both cases.

### 7.3 Open boundaries and uniform degradation

In this case, the model is the same as above, but we have homogeneous Dirichlet boundaries. The solution is given by:

For  $\theta \in [0, \theta_1]$ ,

$$X = \frac{k_0 \sinh(\omega \theta)}{k_d \sinh(\omega)} (\cosh(\omega(1 - \theta_1)) - \cosh(\omega(1 - \theta_2))) \quad (17)$$

For  $\theta \in [\theta_1, \theta_2]$ ,

$$\begin{aligned}X &= \frac{k_0 \sinh(\omega \theta)}{k_d \sinh(\omega)} (\cosh(\omega(1 - \theta)) - \cosh(\omega(1 - \theta_2))) \\ &\quad + \frac{k_0 \sinh(\omega(1 - \theta))}{k_d \sinh(\omega)} (\cosh(\omega \theta) - \cosh(\omega \theta_1))\end{aligned}\quad (18)$$

For  $\theta \in [\theta_2, 1]$ ,

$$X = \frac{k_0 \sinh(\omega(1 - \theta))}{k_d \sinh(\omega)} (\cosh(\omega \theta_2) - \cosh(\omega \theta_1)) \quad (19)$$

where  $\omega = \sqrt{\frac{k_d}{D}}$ .

If we now consider two compartments as before, with constant production localised in one of them, the above solution can be used to once again see that the steady state level in compartment 1 (centred at  $p_1$ ) is related to a production in compartment 2 (centred at  $p_2$  ( $p_1 < p_2$ )) in exactly the same way as the steady state level in compartment 2 is related to a production in compartment 1.

Using (17) we find:

$$\begin{aligned}\langle X \rangle_2 &= \frac{4 \sinh^2(\frac{\omega l}{2}) k_0}{l k_d \omega \sinh(\omega)} \sinh(\omega p_1) \sinh(\omega(1 - p_2)) \\ &= \frac{4 \sinh^2(\frac{\omega l}{2})}{l k_d \omega \sinh(\omega)} \sinh(\omega p_1) \sinh(\omega(1 - p_2)) (\text{Production rate of } X \text{ in compartment 1})\end{aligned}\quad (20)$$

Now consider the case where the production is in compartment 2. Here we use (19) above to calculate the average:

$$\begin{aligned}\langle X \rangle_1 &= \frac{4 \sinh^2(\frac{\omega l}{2}) k_0}{l k_d \omega \sinh(\omega)} \sinh(\omega(1 - p_2)) \sinh(\omega p_1) \\ &= \frac{4 \sinh^2(\frac{\omega l}{2})}{l k_d \omega \sinh(\omega)} \sinh(\omega(1 - p_2) \sinh(\omega p_1)) (\text{Production rate of } X \text{ in compartment 2})\end{aligned}\quad (21)$$

From (20) and (21) above, it is clear that the constant of proportionality multiplying the production rate is the same in both cases.

In all the above cases, the expressions for the solutions have been validated by comparison with steady state concentration profiles obtained by numerical solution of the PDE models, for fixed values of parameters. We also note that the symmetry associated with the relationship between a localised production at one location and the (average) steady state level at another location can also be seen for the Green's functions associated with these boundary value problems.

## 7.4 Adaptation to spatial separation in the uniform channel

The above analysis reveals that for compartments of the same size, in a uniform channel with open or closed boundaries and/or uniform degradation, the steady state level in one compartment is related to a production in a second compartment in exactly the same way as the steady state level in the second compartment is related to a production in the first. This result is analogous to that obtained for the well-mixed compartments (at the beginning of Section 5). The above result can be also exploited in the same way - i.e. through repression - to achieve adaptation to spatial separation in a compartment within a uniform channel. Again this involves promoter saturation, as studied previously. However, we note that while the above results for the compartmental averages are exact irrespective of the size of the compartments, the compartments are not well-mixed. Since the cancellation effect of repression involves a local rather than an average concentration, in the uniform channel this can only be attained in the limit of thin compartments relative to domain size (so that there is no significant disparity between the local concentration and the compartmental average). Note that a compartment close to an open boundary can compromise promoter saturation.

## 7.5 Finding symmetric locations

Using the above solutions, and calculating the spatial average of the concentration profile over potential compartment locations, we see that, for a fixed location of the sender(receiver) compartment, there can be a pair of 'symmetric' locations for the receiver(sender) compartment (i.e. a pair of locations such that placing the receiver(sender) compartment at either one would result in the same average signal level over the receiver compartment). Suppose the sender location (midpoint of the compartment) is at  $p$ , then the symmetric pair of locations  $p_1$  and  $p_2$  (where  $p_1 < p < p_2$ ) are related by:

### Open boundaries and no degradation

$$p_1(1 - p) = p(1 - p_2)$$

### Closed boundaries and uniform degradation

$$\cosh(\omega p) \cosh(\omega(1 - p_2)) = \cosh(\omega p_1) \cosh(\omega(1 - p))$$

In this case, depending on the value of  $p$ , it is possible that a symmetric location corresponding to a given location  $p_1$  may not exist (the expression  $\frac{\cosh(\omega p_1) \cosh(\omega(1 - p))}{\cosh(\omega p)}$  may be less than 1).

## Open boundaries and uniform degradation

$$\sinh(\omega p) \sinh(\omega(1 - p_2)) = \sinh(\omega p_1) \sinh(\omega(1 - p))$$

With open boundaries, a symmetric location  $p_2$  exists for any given  $p$  and  $p_1$  within the domain. Note that the above analysis involves only the locations of the midpoints of the compartments assumes that the size of the compartments is such that they may be placed at these locations without creating an overlap between compartments or crossing the boundaries of the domain. The above expressions relating the symmetric locations have been validated through numerical solution of the PDE models.

**Note:** The above analysis did not consider dimerisation. The full system examined in our study includes a dimer form for each protein, that is also diffusible and subject to degradation. If we consider the case of constant production of  $X$  within a compartment as above, and include dimer formation, transport and degradation, the equations are as follows:

In the  $X$  compartment ( $\theta \in \Omega_X$ ),

$$\begin{aligned} \frac{\partial X}{\partial t} &= k_0 - 2k_X^2 X^2 + 2k_X^{-2} X_2 - k_X^d X + D_X \frac{\partial^2 X}{\partial \theta^2} \\ \frac{\partial X_{dim}}{\partial t} &= k_X^2 X^2 - k_X^{-2} X_{dim} - k_{X_{dim}}^d X_{dim} + D_{X_{dim}} \frac{\partial^2 X_{dim}}{\partial \theta^2} \end{aligned}$$

Outside the  $X$  compartment ( $\theta \notin \Omega_X$ ),

$$\begin{aligned} \frac{\partial X}{\partial t} &= -2k_X^2 X^2 + 2k_X^{-2} X_2 - k_X^d X + D_X \frac{\partial^2 X}{\partial \theta^2} \\ \frac{\partial X_{dim}}{\partial t} &= k_X^2 X^2 - k_X^{-2} X_{dim} - k_{X_{dim}}^d X_{dim} + D_{X_2} \frac{\partial^2 X_{dim}}{\partial \theta^2} \end{aligned}$$

For the purpose of our study, we assume that  $D_X = D_{X_{dim}}$  and  $k_X^d = k_{X_{dim}}^d$  in all cases unless otherwise specified). As seen for the channel between compartments in section 1 above, with these assumptions, multiplying the dimer equation by two and adding this to the monomer equation (both within and outside the compartment) gives us equations for the total concentration of protein  $X_T = X + 2X_{dim}$  ([monomer]+2[dimer]). These equations have the same form as those used in sections 7.1 to 7.3 above. Thus, when we have dimer formation, the above results (i.e pertaining to symmetric locations) can apply to the total amount of protein.

## 8 Effect of membranes bounding compartments

Our model of the uniform 1-D channel does not explicitly incorporate compartment boundaries, and this is reflected in the fact that all proteins can in principle diffuse along the channel. We briefly comment on the effect of membranes and compartment boundaries. By examining a model of spatial organisation in a 1-D channel, involving compartments with boundaries, we find that at steady state, the primary effect of the membrane is to create a possible difference in the concentration gradient of proteins inside and outside the compartment. While this can quantitatively perturb the behaviour of the system, many of the essential qualitative insights - basic trends and design principles - continue to hold good. The presence of a membrane allows for multiple other features - the selective localisation of a component in a compartment, and additional tunable dials for manipulating the transport of species across compartments. The former feature can be incorporated within the existing model in a simple way by localising those species and regarding them as non-diffusible. The latter is beyond the scope of the current study. We note that membraneless compartments encapsulating the transcription-translation process, including coacervate and hydrogel based compartments, have been studied in multiple cell-free contexts, as discussed in the recent review by Dubuc et al. (2019).

## 9 Spatial organisation of degradation

In order to examine the effect of co-localising a common degrading enzyme with the sender or the receiver compartment in a uniform channel, as well as to study the possible distribution of a fixed amount of

this degrading enzyme into the sender and receiver compartments, we consider the scenario shown in Fig. S1(E). We have a source compartment, with co-localised degradation (rate constant  $k_{d1}$ ) and a receiver compartment, also with co-localised degradation (rate constant  $k_{d2}$ ), placed in a uniform 1-D channel with closed boundaries. Both compartments are of equal size  $w_L$ . The model is as follows:

For  $\theta \in (0, \theta_1)$

$$\frac{\partial[X]}{\partial t} = D_X \frac{\partial^2[X]}{\partial \theta^2}$$

For  $\theta \in (\theta_1, \theta_2)$ ,

$$\frac{\partial[X]}{\partial t} = k_0 - k_{d1}X + D_X \frac{\partial^2[X]}{\partial \theta^2}$$

For  $\theta \in (\theta_2, \theta_3)$ ,

$$\frac{\partial[X]}{\partial t} = D_X \frac{\partial^2[X]}{\partial \theta^2}$$

For  $\theta \in (\theta_3, \theta_4)$ ,

$$\frac{\partial[X]}{\partial t} = -k_{d2}X + D_X \frac{\partial^2[X]}{\partial \theta^2}$$

For  $\theta \in (\theta_4, L)$

$$\frac{\partial[X]}{\partial t} = D_X \frac{\partial^2[X]}{\partial \theta^2}$$

With no flux boundary conditions, the solution takes the following form:

$$\begin{aligned} X &= c_1 \quad \text{for } \theta \in (0, \theta_1) \\ X &= \frac{k_0}{k_{d1}} + c_2 \cosh(\omega_1(\theta - \theta_1)) \quad \text{for } \theta \in (\theta_1, \theta_2) \\ X &= c_3\theta + c_4 \quad \text{for } \theta \in (\theta_2, \theta_3) \\ X &= c_5 \cosh(\omega_2(\theta_4 - \theta)) \quad \text{for } \theta \in (\theta_3, \theta_4) \\ X &= c_6 \quad \text{for } \theta \in (\theta_4, L) \end{aligned}$$

where  $\omega_1 = \sqrt{\frac{k_{d1}}{D}}$  and  $\omega_2 = \sqrt{\frac{k_{d2}}{D}}$ . The constants  $c_i$  are given by:

$$\begin{aligned} c_2 &= -\left(\frac{k_0}{k_{d1}}\right) / \left(\cosh(\omega_1 w_L) + \omega_1 \sinh(\omega_1 w_L) \left(\theta_3 - \theta_2 + \frac{\cosh(\omega_2 w_L)}{\omega_2 \sinh(\omega_2 w_L)}\right)\right) \\ c_1 &= \left(\frac{k_0}{k_{d1}}\right) + c_2 \\ c_3 &= c_2 \omega_1 \sinh(\omega_1 w_L) \\ c_5 &= \frac{-c_3}{\omega_2 \sinh(\omega_2 w_L)} = c_6 \end{aligned}$$

We use the above solution to compute spatial averages of the concentration profile over both the 'sender' and 'receiver' compartments, and over the whole domain. These are given by:

$$\begin{aligned} \langle X \rangle_{\text{sender}} &= \frac{1}{w_L} \left( \frac{k_0 w_L}{k_{d1}} + \frac{c_2 \sinh(\omega_1 w_L)}{\omega_1} \right) \\ \langle X \rangle_{\text{receiver}} &= \frac{1}{w_L} \left( \frac{c_5 \sinh(\omega_2 w_L)}{\omega_2} \right) \end{aligned}$$

If the common degrading enzyme is assumed to act via mass action kinetics, then we can use the above solution to analyse the distribution of a fixed amount of enzyme between the sender and receiver compartments. In this case, the degradation rate constants  $k_{d1}$  and  $k_{d2}$  will be proportional to the concentration of enzyme in the respective compartments.

**Note:** The average of the sender signal over the receiver compartment is the same for the cases where all the degrading enzyme is localised at a single location co-localised with the sender or the receiver. To see why, consider the mass balance for the sender species in the whole domain. If the degrading enzyme is co-localised with the sender, then at steady state, the concentration of the sender output is uniform over the whole domain (which is closed), and the mass balance gives us  $k_0 w_L = k_d w_L \langle X \rangle_{sender}$ . Thus, we have  $\langle X \rangle_{receiver} = \langle X \rangle_{sender} = \frac{k_0}{k_d}$ . If the degrading enzyme is co-localised with the receiver, then at steady state, the mass balance gives us  $k_0 w_L = k_d w_L \langle X \rangle_{receiver}$ . Thus, the average of the sender output over the receiver is again  $\langle X \rangle_{receiver} = \frac{k_0}{k_d}$ . We also note that, by the same principle, the average of the sender output over the whole domain is also equal to  $\frac{k_0}{k_d}$  if the same total amount of enzyme is distributed over the whole domain (and assumed to function in the unsaturated regime)

## 9.1 Systems insights applied to a bistable circuit - adaptation to spatial separation

In the discussion, we have briefly described how, for a two node distributed bistable circuit in a uniform channel, localisation of a common degrading enzyme with one of the nodes allows the circuit characteristics to remain unaffected by changing compartment separation. This essentially arises from the fact that the localised degradation of both proteins X and Y (monomers and dimers) at a single location, maintains the average steady state concentration of the monomers at this location, irrespective of where they are produced. In Fig.S4 (A) and (B) we show computational evidence to support this insight, through a bifurcation analysis of the full PDE model (kinetic parameter values used are identical to those used in Figure 2; domain size  $L=10$ , compartment sizes are  $0.1L$ , and the diffusivities (equal for monomers and dimers)  $D = 0.05$  for both nodes). Here we see that the bistable characteristics of the switch are maintained almost exactly in the face of changing compartment separation. In particular, the switching thresholds are essentially unchanged, and so are the (average) steady state concentration of both monomers (X and Y) in the X compartment. Furthermore, on examining the average steady state concentration of the Y monomer in its production compartment, we see that this can be tuned by changing separation - it increases with increasing separation.

## 10 Localised oscillator in a uniform channel: ‘Predator-Prey’ Oscillator

A predator-prey type oscillatory circuit built using the PEN toolbox has been compartmentalised within water-in-oil compartments (Genot et al. 2016). We use a model of this oscillator to examine the basic effects of localising an oscillator in a uniform channel. A simplified model of this oscillator (Genot et al. 2016) is given by:

$$\begin{aligned}\frac{dn}{dt} &= pol.tem.n(1 - \beta.pol.tem.n) - pol.p.n - \lambda.exo \frac{n}{1+p} \\ \frac{dp}{dt} &= pol.p.n - exo \frac{p}{1+p}\end{aligned}$$

where  $n$  and  $p$  are the ‘prey’ and ‘predator’ concentrations,  $\beta$ ,  $\lambda$  are parameters, and  $tem$ ,  $pol$ , and  $exo$  are the (fixed) concentrations of template, DNA polymerase, and exonuclease respectively. The unstable equilibrium point is given by (Genot 2016):

$$\begin{aligned}n_{ss} &= \frac{1 + tem - \sqrt{\Delta}/pol}{2(pol.tem^2.\beta + \lambda)} \\ p_{ss} &= -1 + tem + \frac{\sqrt{\Delta}}{2pol}\end{aligned}$$



The Jacobian for this system of ODEs,  $J_{ij}$  may be calculated as follows:

$$\begin{aligned} J_{11} &= pol.tem(1 - 2 * \beta.pol.tem) - pol.p - \frac{\lambda.exo}{1+p} \\ J_{12} &= -pol.n + \frac{\lambda.exo.n}{(1+p)^2} \\ J_{21} &= pol.p \\ J_{22} &= pol.n - \frac{exo}{(1+p)^2} \end{aligned}$$

We first analyse the behaviour of this system (with parameters chosen in the oscillatory regime) in a spatial configuration involving two well-mixed compartments, with species allowed to diffuse between the compartments. If the time scale of diffusion is assumed to be much faster than the time scale of reactions, the dynamics can be approximately captured by a compartmental model. Through a bifurcation analysis of this compartmental description, we make the following observations: (i) If the whole system (including degradation) is localised in a single compartment and one of the species is allowed to diffuse between compartments, this can destabilise the oscillations and lead to a steady state where the diffusing species is equal in both compartments. (ii) This destabilisation of the oscillations depends on both the diffusivity and the relative sizes of the compartments. (iii) For fixed compartment sizes, starting at a low diffusivity, increasing diffusivity can de-stabilise the oscillations, leading to a stable steady state (through a Hopf bifurcation). Further increase in diffusivity can de-stabilise this steady state, restoring oscillatory behaviour.

Next, we analyse the behaviour of the analogous system in the uniform 1-D channel with closed boundaries. That is, we localise the whole system (all reactions including degradation) to a compartment in the 1-D domain, and let one of the species diffuse across the whole domain. The kinetic parameters are the same as above. We note that, for these parameter values, if the prey species is diffusible, while the predator species is non-diffusible, then in addition to possible oscillatory instability of the homogeneous steady state, the system also has a diffusive instability, with growing non-homogeneous modes. However, since pattern forming behaviour is not the focus of this study, we examine the alternative case, where the predator diffuses and the prey does not. In this case, depending on the size of the compartment relative to the domain, we observe the same qualitative trends as above, for the effect of diffusivity on oscillatory behaviour. Computational results illustrating these trends are shown in Figure 6, and discussed in the main text. We also note that we observed similar behaviour with respect to changing diffusivity and compartment size, in the same spatial configuration (both uniform channel and well-mixed compartments) for other models of chemical oscillators, including (i) the transcription-translation based activator-inhibitor oscillator used in this study (assuming equal degradation of protein and dimer within the compartment, (ii) the Brusselator model (Kuznetsov 2004), (iii) the Oregonator model (Mazzotti et al. 1995).

## 11 Location dependence in a uniform channel: Single production compartment

For a single production compartment located in a uniform channel (see Section 7), the average concentration of the output, (both average over the domain and average over the production compartment), can depend on the location of the compartment within the domain. With open boundaries, both of these measures of output are maximised when the compartment is placed at the centre of the domain, i.e. furthest from the boundaries. With closed boundaries and uniform degradation, only the average over the production compartment exhibits location dependence, while the domain average is independent of the compartment location. Here we use the analytical solutions presented in Section 7, to examine this position dependent behaviour, focussing on the average of the output over the production compartment.

### 11.1 With open boundaries and no degradation

Let the domain size be normalised to 1 and let the compartment of size  $l$  be at location  $p$  (midpoint of the compartment). At steady state, the concentration profile has a constant gradient outside the compartment,

and equals zero at the two boundaries. For simplicity, we will examine the case where the compartment size is small relative to the size of the domain ( $l \ll 1$ ). In this case, the steady concentration profile is relatively flat within the compartment, and can be approximated by its average  $x_c$ . Now, the removal of the species from the compartment happens via diffusion out of the compartment through the boundaries. The steady state mass balance for the compartment thus has the form:

$$lk_0 - R_{\text{boundaries}} = 0$$

where the first term represents localised production and the second term represents the net outflow through the compartment boundaries. From the solution presented in section 7.1, the steady state fluxes at the compartment boundaries are:

$$D \left. \frac{dx}{d\theta} \right|_{\theta_1} = k_0 l (1 - p); \quad D \left. \frac{dx}{d\theta} \right|_{\theta_2} = -k_0 l p,$$

while the average concentration in the compartment (approximated by the concentration at the midpoint) is given by

$$x_c \approx \frac{k_0}{D} l p (1 - p)$$

where the approximation is valid for  $l \ll 1$ . Thus, the net outflow through the compartment boundaries can be expressed as:

$$\begin{aligned} R_{\text{boundaries}} &= D \left. \frac{dx}{d\theta} \right|_{\theta_1} - D \left. \frac{dx}{d\theta} \right|_{\theta_2} \\ &= \frac{D}{p} x_c + \frac{D}{(1-p)} x_c \end{aligned}$$

In this instance, this expression could be obtained directly, exploiting the fact that the boundaries have zero concentrations.

Using this approximation for the effective outflow of the species, the steady state mass balance for the compartment thus has the form:

$$l(k_0 - k_d^{\text{eff}} x_c) = 0$$

where  $k_d^{\text{eff}} = \frac{D}{p(1-p)l}$ . The compartmental average at steady state is therefore given by  $x_c = \frac{k_0}{k_d^{\text{eff}}}$ . Now,  $k_d^{\text{eff}}$  is minimum when  $p = 0.5$  (i.e. the compartment is at the centre of the domain), and increases towards the boundaries. Thus,  $x_c$  must be maximum when the compartment is placed at the centre of the domain.

## 11.2 With closed boundaries and uniform degradation

Proceeding exactly as above, we see that the steady state mass balance for the compartment has the form:

$$lk_0 - lk_d x_c - R_{\text{boundaries}} = 0$$

where the first term represents localised production, the second term represents degradation within the compartment, and the third term represents the net outflow through the compartment boundaries. From the solution presented in section 7.2, for  $l \ll 1$ , the compartmental average (approximated by the concentration at the midpoint) is given by:

$$x_c \approx \frac{2k_0 \sinh(\frac{\omega l}{2}) \cosh(\omega p) \cosh(\omega(1-p))}{k_d \sinh(\omega)}$$

where  $\omega = \sqrt{\frac{k_d}{D}}$ . Again, using the analytical solution and neglecting appropriate terms for  $l \ll 1$ , the total removal rate of the species through the boundaries is approximately given by:

$$\begin{aligned} R_{\text{boundaries}} &\approx \frac{k_0 D \omega \sinh(\omega l)}{k_d \sinh(\omega)} ((\cosh(\omega(1-p)) \sinh(\omega p) + \sinh(\omega(1-p)) \cosh(\omega p)) \\ &= \left[ \frac{D \omega \sinh(\omega l)}{2 \sinh(\frac{\omega l}{2})} \left( \frac{\sinh(\omega p)}{\cosh(\omega p)} + \frac{\sinh(\omega(1-p))}{\cosh(\omega(1-p))} \right) \right] x_c \end{aligned}$$

Note that the above expression for the flux through the boundaries can also be derived by solving two separate boundary value problems, with fixed concentration  $x_c$  at one boundary (left or right) and a closed boundary at the other end.

Using this approximation for the effective outflow of the species, the steady state mass balance for the compartment thus has the form:

$$l(k_0 - k_d^{eff} x_c) = 0$$

where

$$k_d^{eff} = \left[ k_d + \frac{D\omega \sinh(\omega l)}{2l \sinh(\frac{\omega l}{2})} \left( \frac{\sinh(\omega p)}{\cosh(\omega p)} + \frac{\sinh(\omega(1-p))}{\cosh(\omega(1-p))} \right) \right]$$

The compartmental average at steady state is again given by  $x_c = \frac{k_0}{k_d^{eff}}$ . However, in this case, we see that  $k_d^{eff}$  has a minimum when the compartment is placed closed to the boundaries, and is maximum when it is placed at the centre. Thus, in contrast to the previous case,  $x_c$  is maximised by placing the compartment close to the boundaries of the domain.

## 12 Location dependence in a uniform channel: Localizing a bistable motif

Here we examine the localisation in a uniform channel, of the single node, auto-catalytic bistable motif (Gines et al. 2017) discussed in section 4. We again assume that both the autocatalytic template and the ‘pseudo-template’ are co-localised.

### 12.1 Placement in an open domain

With open boundaries (homogeneous Dirichlet BCs), the degrading enzyme is not essential to achieve a steady state since there is a removal of species through the boundaries. We therefore perform the analysis of the PDE model without the degrading enzyme, while noting that qualitatively similar insights hold good if a degrading enzyme is present along with open boundaries. Let the domain size be normalised to 1 and let the compartment of size  $l$  be at location  $p$  (midpoint of the compartment). At steady state, the concentration profile is linear outside the compartment, and equals zero at the two boundaries. For simplicity, we will examine the case where the compartment size is relatively small relative to the size of the domain ( $l \ll 1$ ). In this case, the steady concentration profile is relatively flat within the compartment, and can be approximated by its average  $x_c$ . Now, the removal of the species from the compartment happens in two ways (i) diffusion out of the compartment through the boundaries and (ii) conversion by pseudo-template within the compartment. The steady state mass balance for the compartment thus has the form:

$$l \left( \frac{k_1 x_c}{K_1 + x_c} - \frac{k_2 x_c}{K_2 + x_c} \right) - R_{\text{boundaries}} = 0$$

where the first two terms represent localised production and removal (production from the autocatalytic template and conversion through the pseudo-template, and the last term represents the net outflow through the compartment boundaries. Since the only difference with the system considered in Section 10.1 is inside the compartment, the gradients outside, as a function of the compartment concentration  $x_c$ , remain exactly the same.

Thus, the net outflow through the compartment boundaries can be expressed as:

$$\begin{aligned} R_{\text{boundaries}} &= D \left. \frac{dx}{d\theta} \right|_{\theta_1} - D \left. \frac{dx}{d\theta} \right|_{\theta_2} \\ &= \frac{D}{p} x_c + \frac{D}{(1-p)} x_c \end{aligned}$$

This is obtained by noting that the gradient is a constant, and the boundaries have zero concentration.

Using this approximation for the effective outflow of the species in the present scenario (i.e. the localised bistable motif), the steady state mass balance for the compartment has the form:

$$\frac{k_1 x_c}{K_1 + x_c} - \frac{k_2 x_c}{K_2 + x_c} - k_d^{eff} x_c = 0$$

where  $k_d^{eff} = \frac{D}{p(1-p)l}$ . This equation has the same form as the RHS of (1). Now suppose the kinetic parameters are such that (1) is bistable only for  $k_d < k_d^*$ . This would imply that, in the present scenario, we need  $k_d^{eff} < k_d^*$  for the motif to exhibit bistability. It can be seen that locations within the domain satisfying this condition exist only when  $4D < k_d^* l$ . If this condition is satisfied, then there exists a range of locations in the middle of the domain (and symmetric about the centre of the domain), where the system is bistable.

## 12.2 Placement in an closed domain with uniform degradation

Localising the templates (both the autocatalytic template and the 'pseudo-template') in a domain with closed boundaries, with the degrading enzyme uniformly distributed over the whole domain, creates the possibility that the bistable behaviour of the motif depends on its location within the domain. This is illustrated in the main text (see Figure 6) with the help of bifurcation curves computed by equilibrium continuation for the PDE model. Here we give an analytical argument to support these computational results. We look for an argument that is similar to the ones used above: by approximating the steady state mass balance for the compartment when  $l \ll 1$ , and thereby obtaining an equation for the compartmental average  $x_c$ , that has the same form as the RHS of (1). Proceeding as before, from the analytical solution for a single production compartment given in section 7.2, we find that, for  $l \ll 1$ , this compartmental average is given by

$$x_c \approx \frac{2k_0 \sinh(\frac{\omega l}{2}) \cosh(\omega p) \cosh(\omega(1-p))}{k_d \sinh(\omega)}$$

where  $\omega = \sqrt{\frac{k_d}{D}}$ .

Here we have used the analytical solution shown in section 7.2, and neglected such terms as are consistent with the assumption  $l \ll 1$ . Now, the removal of the species from the compartment happens in two ways (i) diffusion out of the compartment through the boundaries and (ii) conversion by pseudo-template/degradation within the compartment. The diffusive flux out of the compartment equals the diffusivity times the gradient of the concentration profile at the compartment boundaries. Again, using the analytical solution and neglecting appropriate terms for ( $l \ll 1$ ), the total removal rate of the species through the boundaries is approximately given by:

$$\begin{aligned} R_{\text{boundaries}} &\approx \frac{k_0 D \omega \sinh(\omega l)}{k_d \sinh(\omega)} ((\cosh(\omega(1-p)) \sinh(\omega p) + \sinh(\omega(1-p)) \cosh(\omega p)) \\ &= \left[ \frac{D \omega \sinh(\omega l)}{2 \sinh(\frac{\omega l}{2})} \left( \frac{\sinh(\omega p)}{\cosh(\omega p)} + \frac{\sinh(\omega(1-p))}{\cosh(\omega(1-p))} \right) \right] x_c \end{aligned}$$

When  $l \ll 1$ , this simplifies to

$$R_{\text{boundaries}} = \left[ D \omega \left( \frac{\sinh(\omega p)}{\cosh(\omega p)} + \frac{\sinh(\omega(1-p))}{\cosh(\omega(1-p))} \right) \right] x_c$$

The expression for  $R_{\text{boundaries}}$  as a function of  $x_c$  can also be obtained by solving two boundary value problems (diffusion-degradation), with one boundary at value  $x_c$  and the other boundary insulated. This yields exactly the same result (the solution in each segment being  $x_c \frac{\cosh(\omega \theta)}{\cosh(\omega p)}$  and  $x_c \frac{\cosh(\omega(1-\theta))}{\cosh(\omega(1-p))}$ )

This means that the steady state equation for  $x_c$  can again be approximately expressed in the form:

$$\frac{k_1 x_c}{K_1 + x_c} - \frac{k_2 x_c}{K_2 + x_c} - k_d^{eff} x_c = 0$$

where

$$k_d^{eff} = \left[ k_d + \frac{D\omega \sinh(\omega l)}{2l \sinh(\frac{\omega l}{2})} \left( \frac{\sinh(\omega p)}{\cosh(\omega p)} + \frac{\sinh(\omega(1-p))}{\cosh(\omega(1-p))} \right) \right]$$

The term in square brackets forms an ‘effective’ rate constant of degradation within the compartment, again leaving us with a steady state equation having the same form as the RHS of (1). This term varies symmetrically as  $p$  ranges from 0 to 1 - it has a maximum for  $p = 0.5$  i.e. when the compartment is at the centre of the domain, and is minimum at  $p = 0$  and  $p = 1$ . This implies that it is possible that, for fixed kinetic parameters, the motif may be bistable when the compartment is placed closer to the ends of the domain, and lose bistability when the compartment is closer to the centre of the domain (due to the higher ‘effective’ degradation rate). Although the above analysis assumes  $l \ll 1$ , we note that this behaviour (position dependent bistability) is observed computationally through bifurcation analysis of the PDE model, for a compartment of size  $l = 0.1$  (Fig. 6(A)). Here we use a constant (zeroth order) production of the species as an ‘input’ to the motif (i.e. the bifurcation parameter).

This type of position dependent behaviour, of a bistable motif in the uniform channel, is also seen (computationally) for a transcription translation motif of the type studied here (single node self activation), with uniform (and equal) degradation of both monomer and dimer forms across the domain. This means that the above insights may continue to hold good even in the presence of dimer formation and leak/degradation/transport of dimer.

### 13 Application: Communication with a target

For our analysis of circuit placement relative to a target, we consider a uniform 1-D channel configuration. We make the following basic assumptions: (i) Closed boundaries for the domain, with the target adjacent to one of the boundaries (target location  $p_T$  close to 1). (ii) Small compartment sizes ( $size = l$ ) relative to the size of the domain. This allows us to: (a) approximate the average concentration of a species within a compartment by its concentration at the midpoint of the compartment, and (b) approximate the average production rate using the local form of the kinetic expression, with the local concentration of the activator/inhibitor replaced with its compartmental average. (iii) Spatially uniform degradation rate constants for all diffusing species. (iv) Monomeric regulation for both the action of the inhibitor and the regulation of one node by the other within the synthetic circuit (v) Constant production rate of the inhibitor at the target location (zeroth-order reaction). Note that there is no feedback interaction between the circuit and the target.

For a given location of the circuit, we focus on the steady state concentration of the circuit output at the target location. The circuit output is labelled  $X$ , the target  $T$ , and the inhibitor  $Z$  (see Fig. 7 in the main text). The steady state concentration profiles calculated in Section 7 above can be used to calculate both the level of the inhibitor at the circuit location, and subsequently, the circuit output at the target location. For fixed target location  $p_T$  (midpoint of target region) and variable circuit location  $p_X$ , the level of the inhibitor at the circuit location takes the form:

$$Z(p_X) = f_Z(\omega_Z) \cosh(\omega_Z p_X)$$

$$\text{where } f_Z(\omega_Z) = \frac{2k_Z \cosh(\omega_Z(1-p_T)) \sinh\left(\frac{\omega_Z l}{2}\right)}{k_Z^d \sinh(\omega_Z)}$$

The resulting production rate of  $X$  takes the form  $\frac{k_x}{K_x + Z(p_X)}$ . Thus, the steady state level of  $X$  at the target location exhibits the following dependence on circuit location  $p_X$ :

$$X(p_T) = \frac{f_X(\omega_X) \cosh(\omega_X p_X)}{K_X + f_Z(\omega_Z) \cosh(\omega_Z p_X)}$$

$$\text{where } f_X(\omega_X) = \frac{2k_X \cosh(\omega_X(1-p_T)) \sinh\left(\frac{\omega_X l}{2}\right)}{k_X^d \sinh(\omega_X)}$$

On examining the expression for  $\frac{dX(p_T)}{dp_X}$ , and considering its Taylor series expansion in terms of  $\omega_X$ , we see that the leading order term is negative. This indicates that, for small  $\omega_X$  (and therefore  $\omega_X$  small relative to  $\omega_Z$ ),  $X(p_Z)$  is maximised by lowering  $p_X$ , i.e. ensuring maximum separation from the target. Similarly, by examining the Taylor series expansion of  $\frac{dX(p_T)}{dp_X}$  in terms of  $\omega_Z$ , we see that the leading order term is positive. This indicates that, for  $\omega_Z$  small relative to  $\omega_X$ ,  $X(p_Z)$  is maximised by increasing  $p_X$ , i.e. by co-localising with the target. This confirms the intuitive understanding of how  $\omega_X$  and  $\omega_Z$  determine optimal circuit placement (see text).

Next we examine the two node circuit with no inhibition (the second node is labelled Y). Here (assuming  $p_X$  fixed and  $p_X \leq p_Y$ ), we have the following expressions for X at the location of node Y, and for Y at the target location

$$\begin{aligned} X(p_Y) &= \frac{2k_X \cosh(\omega_X(1 - p_Y)) \sinh\left(\frac{\omega_X l}{2}\right)}{k_X^d \sinh(\omega_X)} \cosh(\omega_X p_X) \\ Y(p_T) &= \frac{2k_Y \cosh(\omega_Y(1 - p_T)) \sinh\left(\frac{\omega_Y l}{2}\right)}{k_Y^d \sinh(\omega_Y)} \cosh(\omega_Y p_Y) \\ \text{where } k_Y &= \frac{k_{0Y} X(p_Y)}{K_Y + X(p_Y)} \end{aligned}$$

Here again, by examining the Taylor series expansions of  $\frac{dY(p_T)}{dp_Y}$  in terms of  $\omega_Y$  and  $\omega_X$ , we see that for  $\omega_Y$  small relative to  $\omega_X$ ,  $Y(p_T)$  is maximised by minimising  $p_Y$  (i.e. co-localising the two circuit nodes), while for  $\omega_X$  small relative to  $\omega_Y$ , it is maximised by increasing  $p_Y$  (i.e. co-localising node Y with the target).

Now, in the case of the two node circuit with inhibition of the first node, Y at the target location again takes the form:

$$\begin{aligned} Y(p_T) &= \frac{2k_Y \cosh(\omega_Y(1 - p_T)) \sinh\left(\frac{\omega_Y l}{2}\right)}{k_Y^d \sinh(\omega_Y)} \cosh(\omega_Y p_Y) \\ \text{where } k_Y &= \frac{k_{0Y} X(p_Y)}{K_Y + X(p_Y)} \end{aligned}$$

Here  $X(p_Y)$  is given by:

$$\begin{aligned} X(p_Y) &= \frac{f_X(\omega_X) \cosh(\omega_X(1 - p_Y)) \cosh(\omega_X p_X)}{K_X + f_Z(\omega_Z) \cosh(\omega_Z p_X)} \\ \text{where } f_X(\omega_X) &= \frac{2k_X \sinh\left(\frac{\omega_X l}{2}\right)}{k_X^d \sinh(\omega_X)} \end{aligned}$$

where the expression for  $Z(p_X)$  is exactly as in the first case (single node circuit with inhibition).

Similar to the two previous cases, here we examine Taylor series expansions of both  $\frac{\partial Y(p_T)}{\partial p_X}$  and  $\frac{\partial Y(p_T)}{\partial p_Y}$ , in terms of  $\omega_Z$ ,  $\omega_X$ , and  $\omega_Y$ . By examining the leading order terms in each case, we see that: (i) for  $\omega_Z$  much smaller than the others,  $Y(p_T)$  is maximised by maximising  $p_X$  and  $p_Y$ , (ii) for  $\omega_X$  much smaller than the others,  $Y(p_T)$  is maximised by maximising  $p_Y$  and minimising  $p_X$ , (i) for  $\omega_Y$  much smaller than the others,  $Y(p_T)$  is maximised by minimising  $p_X$  and  $p_Y$ .

The above results are validated by comparison to computational results. Computational results also indicate that these insights continue to hold good even for larger compartment sizes. For illustrative purposes, we also show computational results for the case involving inhibition of both nodes.

## 14 Retroactive effect in a uniform 1-D channel:

To demonstrate the basic trends associated with spatial organisation and the retroactive effect of an output protein binding to a downstream promoter, we examine a two-node system in a uniform 1-D channel, with

closed boundaries and uniform degradation (Fig. S3). The protein X is produced in a compartment at location  $L_1$ , and diffuses across the domain. The template for the node Y is localised in a compartment at location  $L_2$ . X binds with the promoter sites on the Y template to form a complex  $P_X$ . We consider a production rate of X that varies sinusoidally in time, and examine the dynamics of the protein X and the complex, as in Del Vecchio et al. (2008). The model is as follows:

In the X compartment

$$\frac{\partial X}{\partial t} = k_x - k_d X + D_X \frac{\partial^2 X}{\partial \theta^2}$$

Outside the two compartments

$$\frac{\partial X}{\partial t} = -k_d X + D_X \frac{\partial^2 X}{\partial \theta^2}$$

In the Y compartment

$$\begin{aligned} \frac{\partial X}{\partial t} &= -k_b(P_T - P_X)X + k_u P_X - k_d X + D_X \frac{\partial^2 X}{\partial \theta^2} \\ \frac{\partial P_X}{\partial t} &= k_b(P_T - P_X)X - k_u P_X \end{aligned}$$

where  $P_T$  is the total concentration of promoter, and  $k_x = 0.05(1 + \sin(\omega t))$ , with  $\omega = 0.005$ . On examining the dynamic variation of X concentration at its production compartment, we find that binding to the Y promoter distorts both the amplitude and phase of the oscillations, relative to the case where the Y template is absent (X in isolation). We observe that, depending on the diffusivity, this distortion may be reduced, as the Y compartment is moved away from the X compartment (see Fig. S3). For fixed kinetic parameters, this effect is more pronounced at low diffusivity, and is negligible at high diffusivity.

## 15 Parameters

The parameter values used in the study (including those used in the computational results presented) are presented in the table below. The values of transcription, translation, and degradation rate constants are in ranges taken from the literature, while the rate constants of the dimer reactions and the binding/unbinding reactions to the promoters, are assumed to take relatively larger values, as has been done elsewhere in the literature. In these cases, the rates are chosen so that the equilibrium constants are within ranges described in the literature. The concentrations are assumed to be scaled by a factor of 1 nM, and time by a factor of 1 min.

### 15.1 Spatial Parameters

We assume diffusivities to be of the order of  $10^3 \mu\text{m}^2/\text{min}$ , as described in the literature (Karzbrun et al. 2014). The well-mixed compartments are assumed to have a radius of  $50 \mu\text{m}$ , with channel width ranging from 1 to  $10 \mu\text{m}$ . Lengths are assumed to be scaled by a factor of  $50 \mu\text{m}$ .

## References

- Bleris, L., Xie, Z., Glass, D., Adadey, A., Sontag, E. & Benenson, Y. (2011), ‘Synthetic incoherent feedforward circuits show adaptation to the amount of their genetic template’, *Molecular Systems Biology* **7**(1).  
**URL:** <http://msb.embopress.org/content/7/1/519.abstract>
- Del Vecchio, D., Ninfa, A. J. & Sontag, E. D. (2008), ‘Modular cell biology: retroactivity and insulation’, *Molecular Systems Biology* **4**(1).  
**URL:** <http://msb.embopress.org/content/4/1/161.abstract>
- Dubuc, E., Pieters, P. A., van der Linden, A. J., van Hest, J. C. M., Huck, W. T. S. & de Greef, T. F. A. (2019), ‘Cell-free microcompartmentalised transcription–translation for the prototyping of synthetic

communication networks', *Current Opinion in Biotechnology* **58**, 72–80.

**URL:** <http://www.sciencedirect.com/science/article/pii/S0958166918301629>

Genot, A. J., Baccouche, A., Sieskind, R., Aubert-Kato, N., Bredeche, N., Bartolo, J. F., Taly, V., Fujii, T. & Rondelez, Y. (2016), 'High-resolution mapping of bifurcations in nonlinear biochemical circuits', *Nature Chemistry* **8**, 760.

**URL:** <http://dx.doi.org/10.1038/nchem.2544>

Gines, G., Zadorin, A. S., Galas, J. C., Fujii, T., Estevez-Torres, A. & Rondelez, Y. (2017), 'Microscopic agents programmed by dna circuits', *Nature Nanotechnology* **12**, 351.

**URL:** <http://dx.doi.org/10.1038/nnano.2016.299>

Karzbrun, E., Tayar, A. M., Noireaux, V. & Bar-Ziv, R. H. (2014), 'Programmable on-chip dna compartments as artificial cells', *Science* **345**(6198), 829.

**URL:** <http://science.sciencemag.org/content/345/6198/829.abstract>

Kuznetsov, Y. A. (2004), *Elements of applied bifurcation theory*, 3rd edn, Springer, New York.

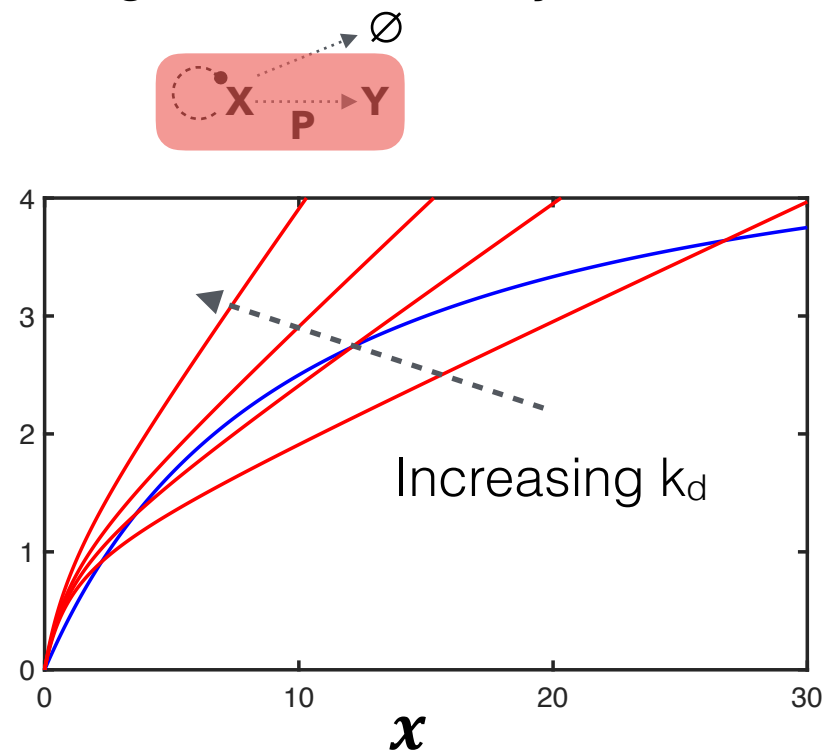
Mazzotti, M., Morbidelli, M. & Serravalle, G. (1995), 'Bifurcation analysis of the oregonator model in the 3-d space bromate/malonic acid/stoichiometric coefficient', *The Journal of Physical Chemistry* **99**(13), 4501–4511.

**URL:** <https://doi.org/10.1021/j100013a020>

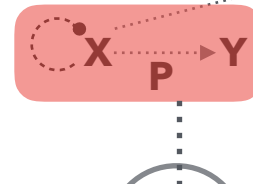
Qian, Y., Huang, H.-H., Jiménez, J. I. & Del Vecchio, D. (2017), 'Resource competition shapes the response of genetic circuits', *ACS Synthetic Biology* **6**(7), 1263–1272.

**URL:** <https://doi.org/10.1021/acssynbio.6b00361>



**Figure S1****A Single node auto-catalytic motif: Bistability****B**

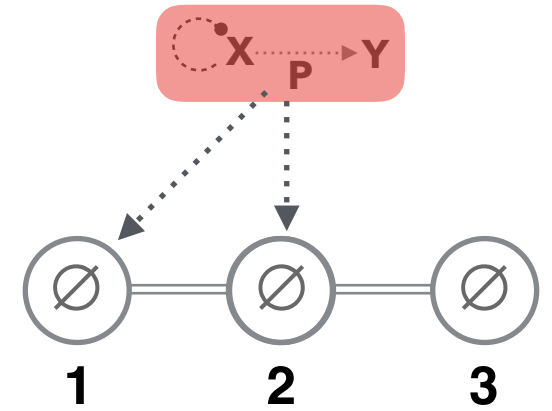
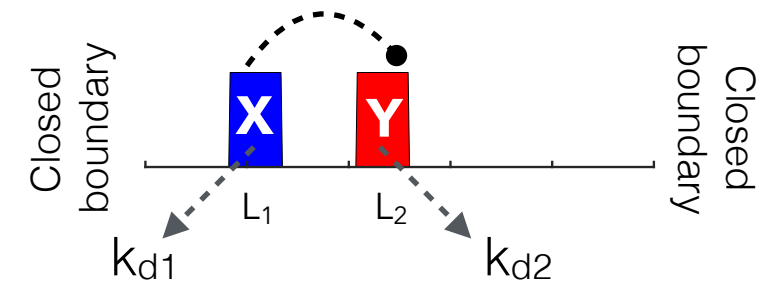
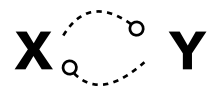
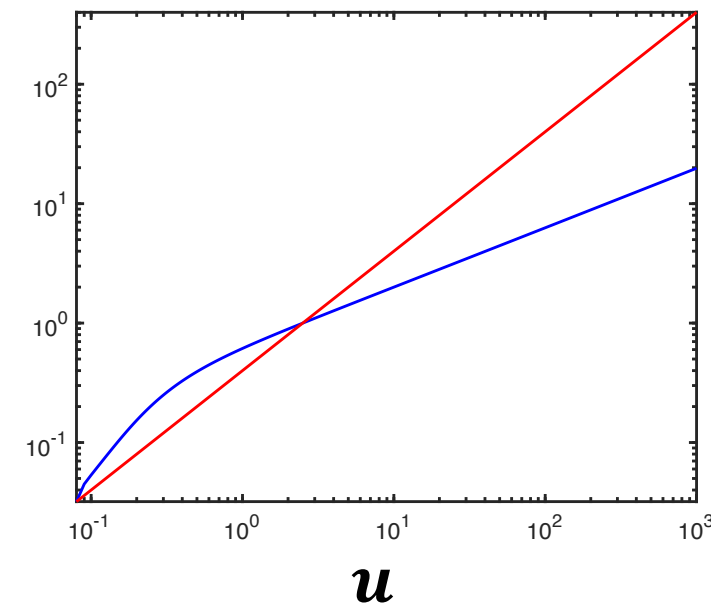
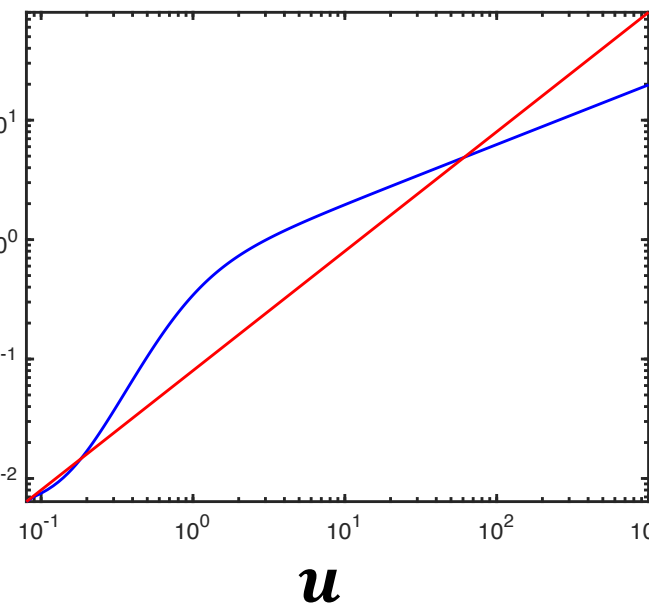
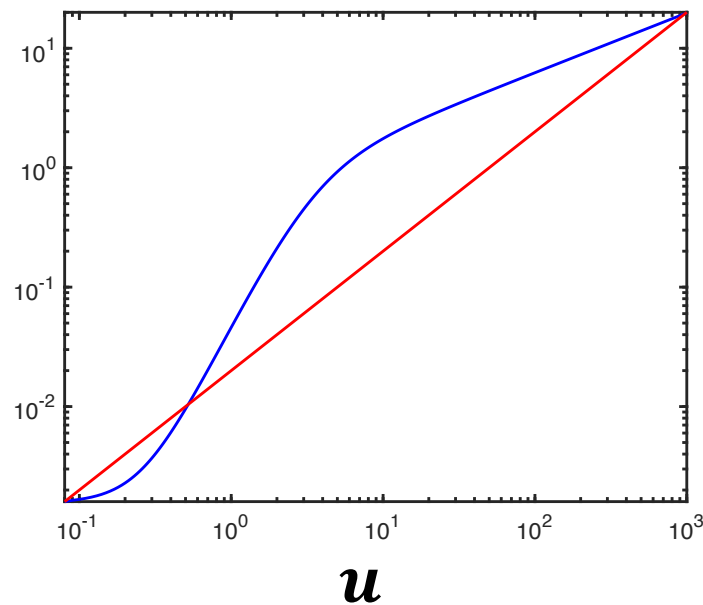
Localising templates



Localising degrading enzyme

**C**

Localising in an array of compartments

**E****D Two node mutual inhibition: Bistability**Increasing  $k_d$ 

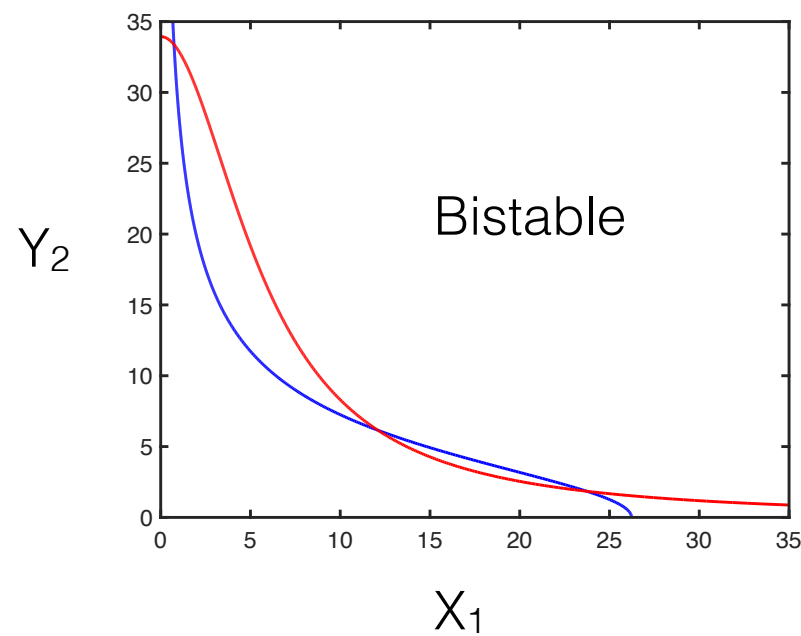
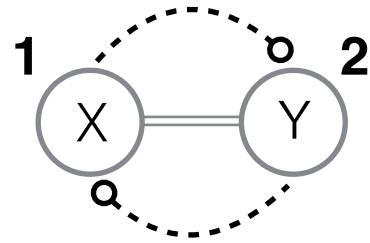
$f_1(u)$   
 $f_2(u)$

**Figure S1: (A)** ODE analysis of the single node autocatalytic motif (Supplemental section 4). Increasing  $k_d$  takes the system out of the bistable regime. **(B)** Schematic for supplemental section 4.1 **(C)** Schematic for supplemental section 4.2; the templates can be localised in the middle compartment or in one of the terminal compartments. **(D)** ODE analysis of the two-node mutual inhibition motif (Supplemental section 4.3). Increasing  $k_d$  takes the system out of the bistable regime. **(E)** Schematic for Supplemental section 8.

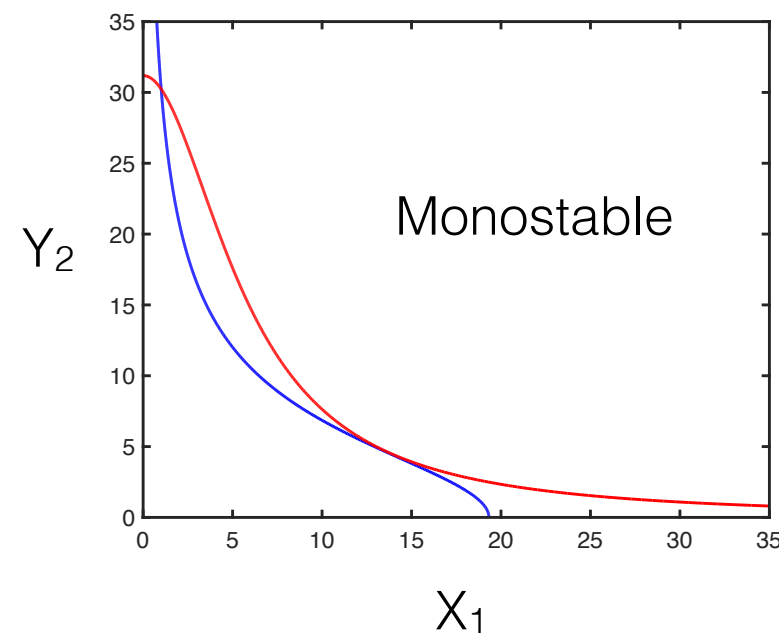
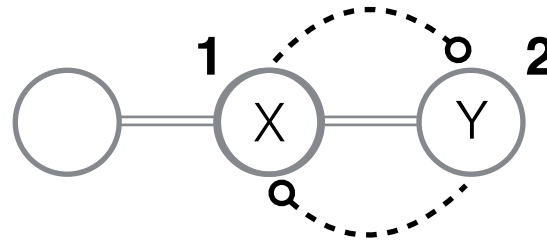
# Modular augmentation

**Figure S2**

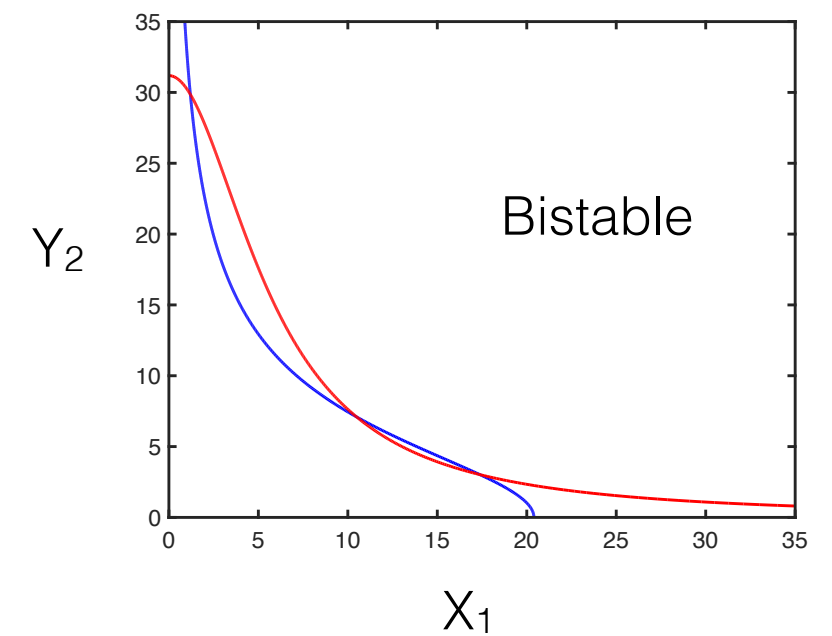
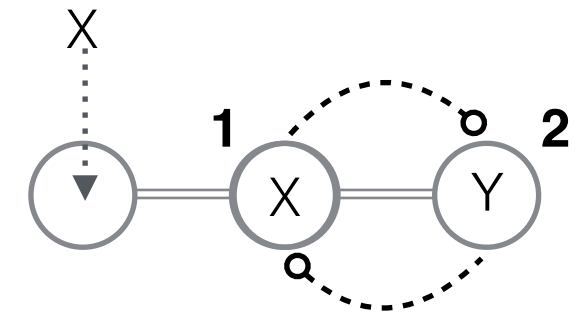
**Two node mutual inhibition:  
Two compartment configuration**



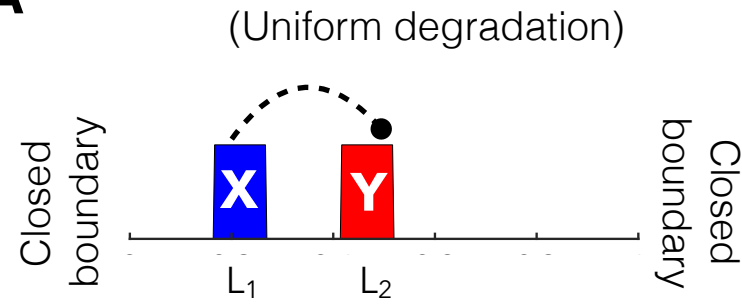
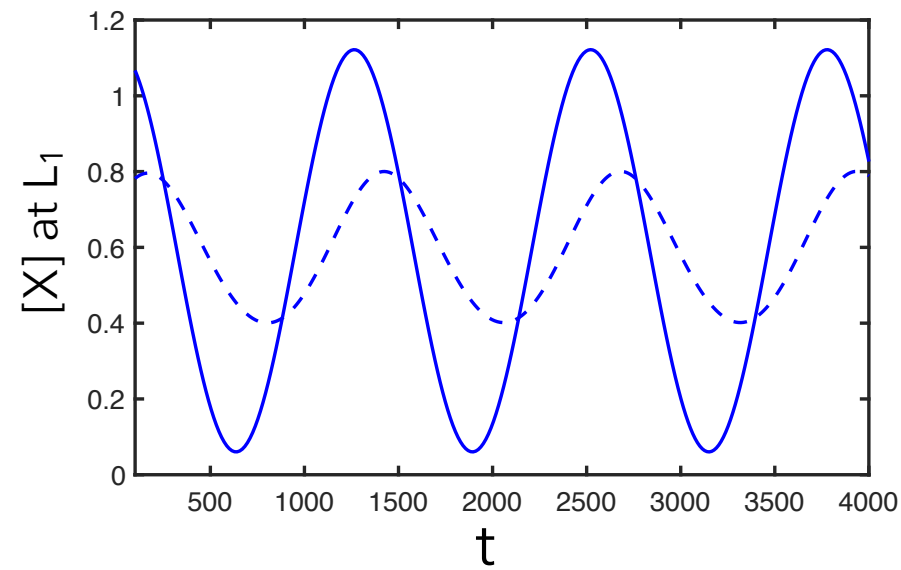
**Connecting to an 'output'  
compartment**



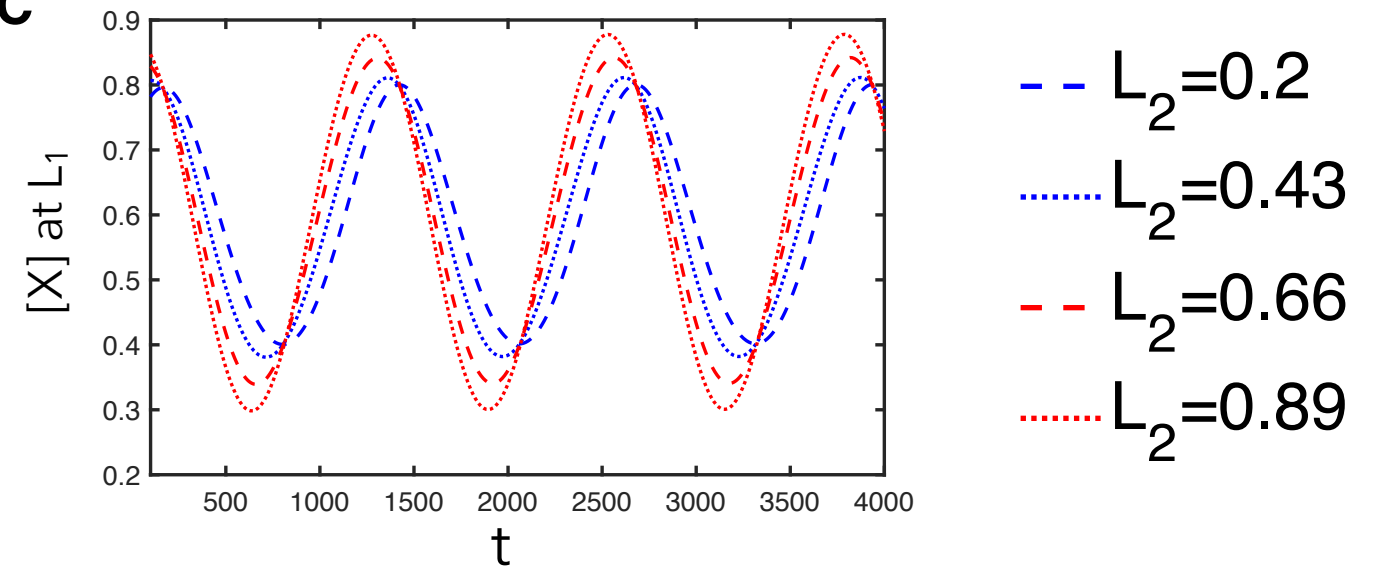
**Connecting to an 'output'  
compartment already containing  
a certain amount of X template**



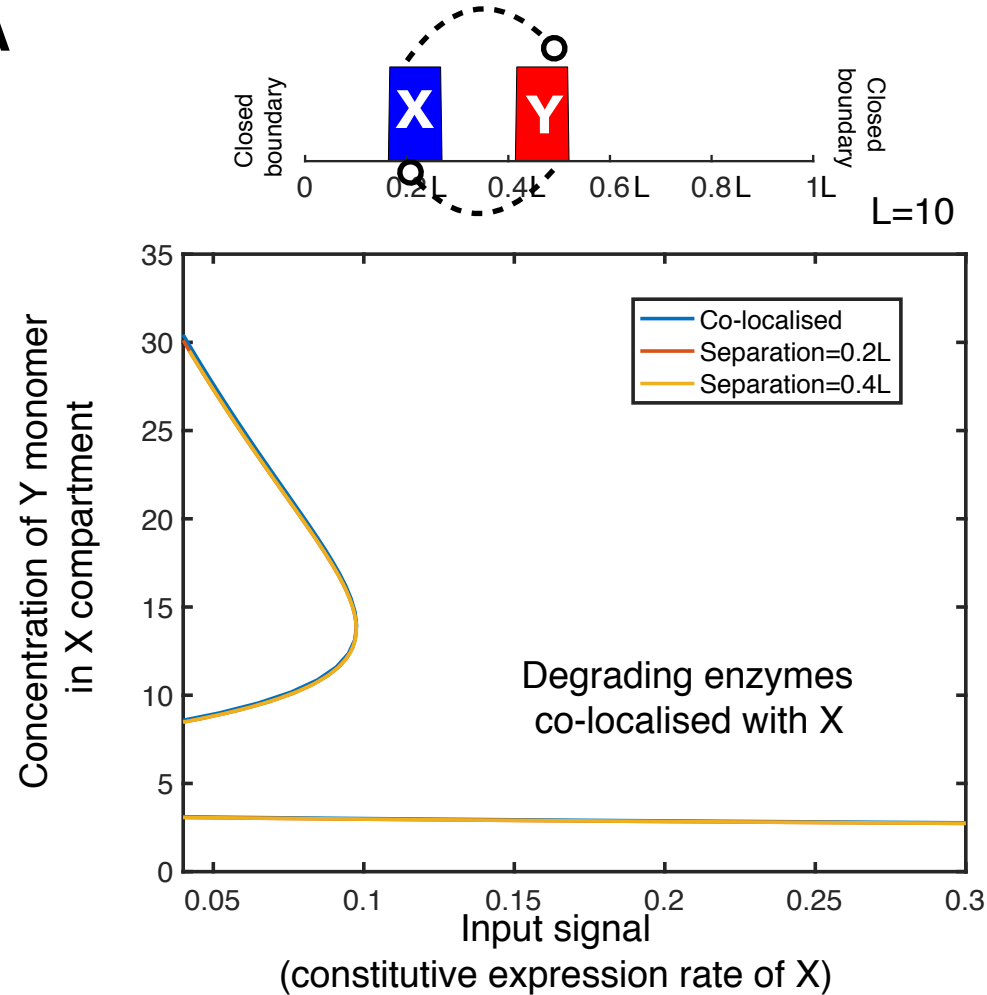
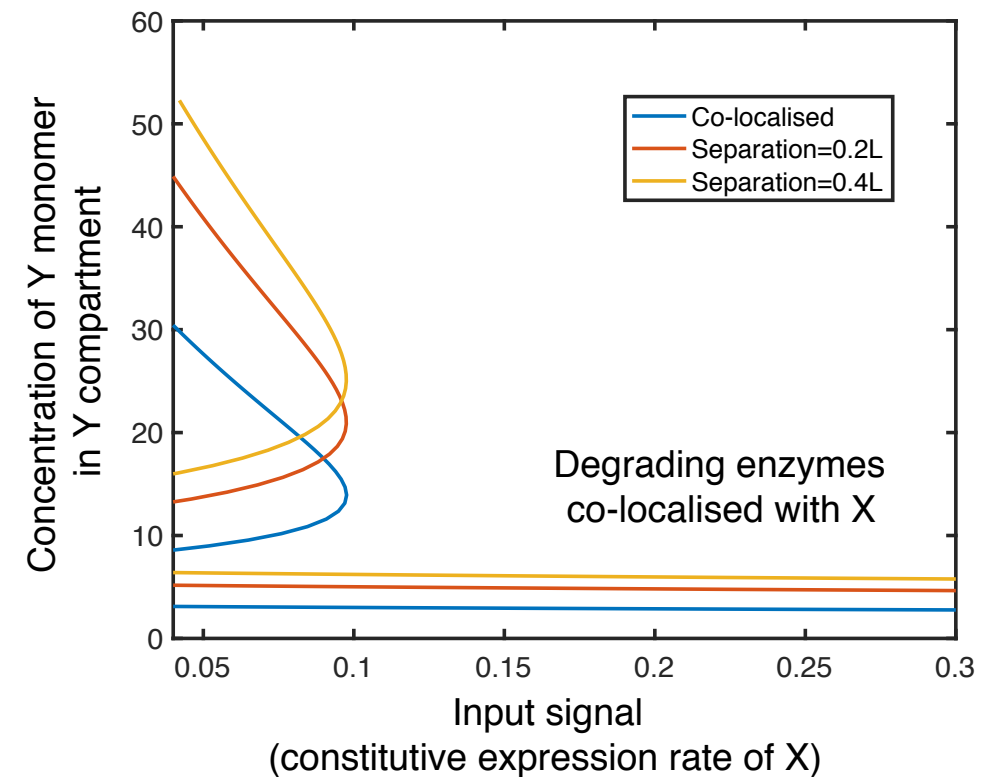
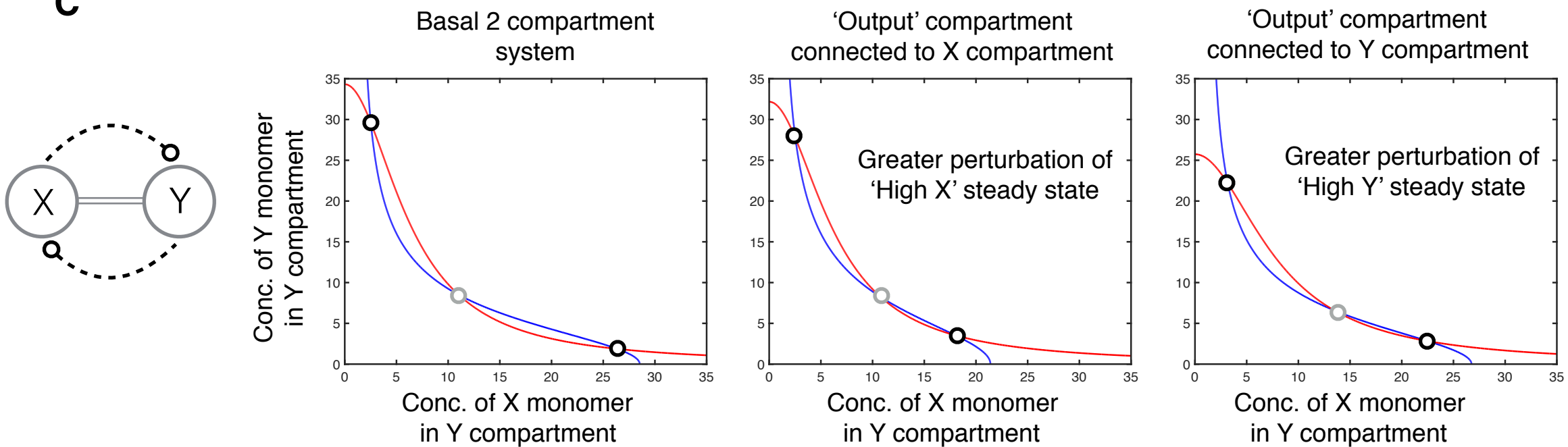
**Figure S2:** Modular augmentation of a two-node distributed bistable circuit (Supplemental section 3.1). The blue and red curves represent null-clines plotted for the simplified model.

**Figure S3****A****B**

— X in isolation  
 - -  $L_1=L_2=0.2$

**C**

**Figure S3:** Effect of spatial separation on retroactivity. **(A)** Schematic of the spatial configuration: uniform 1-D channel with closed boundaries and uniform degradation. X produced (sinusoidal production rate) in a compartment at location  $L_1$ . X reversibly binds to Y template placed in a second compartment at location  $L_2$ . **(B)** Distortion in X oscillations at location  $L_1$ , when Y template is co-localised with X. Both amplitude and phase are affected. **(C)** The distortion caused by the binding to Y template is reduced as the Y compartment is moved away from the X compartment.

**A****Figure S4****B****C**

**Figure S4: (A) and (B)** Two-node bistable circuit in a uniform channel: co-localising degrading enzymes with one of the nodes allows adaptation to spatial separation combined with bistability. **(A)** The switching threshold for the bistable circuit is essentially unaffected by changing separation between X and Y. Furthermore, the steady state concentrations of Y monomer in the X compartment (averaged), are also maintained. **(B)** However, the (average) steady state concentrations of Y monomer at its production compartment are seen to increase with increasing separation. **(C)** Modular augmentation of a distributed bistable circuit - the extent to which different steady states are perturbed depends on where the output compartment is connected (parameter values as used in Figure 3).

# Tables of parameter values used

Figure 2

Well-mixed configuration: Spatial parameters

Spatial Parameters	For oscillators	For all other figures
A (Channel cross-section)	0.2h	0.02h
V (Compartment volume)	$\pi h$	$\pi h$

h is the ‘depth’ of the spatial configuration, uniform across compartments and channels.

A

Node	X	Y
P <sup>T</sup>	6	10.5
k <sup>b</sup>	-	100
k <sup>u</sup>	-	100
k <sup>t</sup>	0.1	0.1
k <sup>d</sup>	0.02	0.02
k <sup>2</sup>	10	10
k <sup>-2</sup>	100	100
r <sup>0</sup>	1.7	2E-04
r <sup>TF</sup>	-	1.1
r <sup>d</sup>	0.1	0.1
D	0.4	0.4
r <sup>const</sup>	-	-

B

Node	X	Y
P <sup>T</sup>	6	10.5
k <sup>b</sup>	-	100
k <sup>u</sup>	-	100
k <sup>t</sup>	0.1	0.1
k <sup>d</sup>	0.02	0.02
k <sup>2</sup>	10	10
k <sup>-2</sup>	100	100
r <sup>0</sup>	1.7	1.1
r <sup>TF</sup>	-	2E-04
r <sup>d</sup>	0.1	0.1
D	0.4	0.4
r <sup>const</sup>	-	-

C

Node	X	Y
P <sup>T</sup>	6	8
k <sup>b</sup>	100	100
k <sup>u</sup>	100	100
k <sup>t</sup>	0.1	0.1
k <sup>d</sup>	0.02	0.02
k <sup>2</sup>	10	10
k <sup>-2</sup>	100	100
r <sup>0</sup>	2E-04	2E-04
r <sup>TF</sup>	1.7	1.3
r <sup>d</sup>	0.1	0.1
D	0.4	0.4
r <sup>const</sup>	0.3	-

D

Node	X	Y
P <sup>T</sup>	6	8
k <sup>b</sup>	100	100
k <sup>u</sup>	100	100
k <sup>t</sup>	0.1	0.1
k <sup>d</sup>	0.02	0.02
k <sup>2</sup>	10	10
k <sup>-2</sup>	100	100
r <sup>0</sup>	1.7	1.3
r <sup>TF</sup>	2E-04	2E-04
r <sup>d</sup>	0.1	0.1
D	0.4	0.4
r <sup>const</sup>	-	-

E,F,G,H

Node	X	Y
P <sup>T</sup>	6	10.5
k <sup>b</sup>	100	-
k <sup>u</sup>	100	-
k <sup>t</sup>	0.1	0.1
k <sup>d</sup>	0.02	0.02
k <sup>2</sup>	10	100
k <sup>-2</sup>	100	100
r <sup>0</sup>	1.7	1.1
r <sup>TF</sup>	2E-04	-
r <sup>d</sup>	0.1	0.1
D	0.4	0.4
r <sup>const</sup>	-	-

Figure 3

Node	X	Y
P <sup>T</sup>	6	8
k <sup>b</sup>	100	100
k <sup>u</sup>	100	100
k <sup>t</sup>	0.1	0.1
k <sup>d</sup>	0.02	0.02
k <sup>2</sup>	10	10
k <sup>-2</sup>	100	100
r <sup>0</sup>	1.7	1.3
r <sup>TF</sup>	2E-04	2E-04
r <sup>d</sup>	0.1	0.1
D	0.4	0.4
r <sup>const</sup>	-	-

Basal Parameter values for bistable mutual inhibition motif. Parameters for simplified model obtained from the above, using a quasi-steady state approximation for dimer formation and binding to promoter.

Figure 4

A to E

Node	All nodes
$P^T$	5, 20
$k^b$	100
$k^u$	15
$k^t$	0.5
$k^d$	0.054
$k^2$	10
$k^{-2}$	1E+03
$r^0$	0.4
$r^{TF}$	0
$r^d$	0.087
$D$	0.4

Basal Parameter values for repressilator motif (Niederholtmeyer et al. 2015)

Node	All nodes
$P^T$	1
$k^b$	100
$k^u$	15
$k^t$	6.93
$k^d$	0.0693
$k^2$	10
$k^{-2}$	1E+04
$r^0$	29.97
$r^{TF}$	0.03
$r^d$	0.347
$D$	0.4

Second set of parameter values for repressilator motif (Elowitz 2000, Biomodels Database)

F

Node	X	Y
$P^T$	4	1
$k^b_X$	100	100
$k^u_X$	1000	1000
$k^b_Y$	1000	-
$k^u_Y$	100	-
$k^t$	1	1
$k^d$	0.2	0.2
$k^2$	100	1000
$k^{-2}$	1000	1000
$r^0$	0.02	2E-04
$r^X$	5	10
$r^Y$	2E-04	-
$r^d$	1	1
$D$	0.4	0.4

Basal parameter values for activator inhibitor oscillator. Template concentration increased by a factor of 150 to obtain sustained oscillations in the two-compartment distributed configuration.

G

Node	X	Y
$P^T$	2	1
$k^b$	100	1
$k^u$	100	100
$k^t$	0.1	0.1
$k^d$	0.02	0.02
$k^2$	10	10
$k^{-2}$	100	100
Transcription rate const.	1.7	1.1
$r^d$	0.1	0.1
$D$	0.4	0.4
$r_{const}$	-	-
Total RNAP	1	
RNAP binding inactive promoter	1E-02	
RNAP binding active promoter	10	
RNAP unbinding	1	

Figure 5

A

Node	X	Y
$\mathbf{p^T}$	6	10.5
$\mathbf{k^b}$	-	100
$\mathbf{k^u}$	-	100
$\mathbf{k^t}$	0.1	0.1
$\mathbf{k^d}$	0.02	0.02
$\mathbf{k^2}$	10	10
$\mathbf{k^{-2}}$	100	100
$\mathbf{r^0}$	1.7	2E-04
$\mathbf{r^{TF}}$	-	1.1
$\mathbf{r^d}$	0.1	0.1
$\mathbf{D}$	0.1	0.1
$\mathbf{r^{const}}$	-	-
Boundaries	Homogeneous Dirichlet	

B

Node	X
$\mathbf{k_0}$	1
$\mathbf{k_d}$	2
$\mathbf{D}$	0.1
Domain Size	1
Compartment Size	0.1
Sender Location	0.2
Receiver Location	0.6
Boundaries	Homogeneous Dirichlet

C,D

Node	X
$\mathbf{k_0}$	1
$\mathbf{k_d}$	2
$\mathbf{D}$	0.1
Domain Size	1
Compartment Size	0.1
Sender Location	0.4
Receiver Location	0.2
Boundaries	Homogeneous Dirichlet

F

Node	X
$\mathbf{k_0}$	0.5
$\mathbf{k_d}$	1
$\mathbf{D}$	1e-4 to 10
Domain Size	1
Compartment Size	0.1
Boundaries	No-flux and Homogeneous Dirichlet

G

Node	X
$\mathbf{k_0}$	0.5
$\mathbf{k_d}$	1
$\mathbf{D}$	1e-4 to 10
Domain Size	1
Compartment Size	0.1
Boundaries	No-flux

Figure 6

A

Node	X
k <sub>1</sub>	5
K <sub>1</sub>	10
k <sub>2</sub>	1
K <sub>2</sub>	1
k <sub>d</sub>	0.03
D	1E-02
Domain Size	1
Compartment Size	0.1
Compartment Locations	0.08, 0.22, 0.38,0.5
Boundaries	No-flux

Basal Parameter values for autocatalytic bistable motif.

B

Parameter	Value
$\beta$	0.12
$\lambda$	4.1
tem	2.1
exo	0.36
pol	0.8
D	1E-3 to 10
Domain Size	1
Compartment Size	5/6, 1/3
Compartment Location	0.5
Boundaries	No-flux

Basal Parameter values for ‘Predator-Prey’ oscillator (in ranges taken from Genot et al. 2016). Initial conditions for all simulations, including ODE, obtained by adding a small perturbation to the unstable equilibrium point.

C,E

Node	X
k <sub>x</sub>	0.2
k <sub>d</sub>	2
k <sub>y</sub>	0.5
D	0.01
Domain Size	1
Compartment Size	0.1
Sender Location	0.15
Receiver Location	0.75
Boundaries	No-flux

D

Node	X
k <sub>x</sub>	0.2
k <sub>d</sub>	2
k <sub>y</sub>	0.5
D	0.01
Domain Size	1
Compartment Size	0.1
Sender Location	0.15
Sink Location	0.35, 0.45, 0.55
Boundaries	No-flux



Figure 7

A

	Node X	Inhibitor Z
k	8.7E+03	1.1E+04
k <sup>d</sup>	1	1
ω	9	10
K	0.8	-
Compartment Size/ Size of production region	0.05	0.05
Domain size	1	
Location	-	0.975

	Node X	Inhibitor Z
ω	1	0.1

	Node X	Inhibitor Z
ω	0.1	1

B

	Node X	Node Y
k	8.7E+03	5.4E+03
k <sup>d</sup>	1	1
ω	3	2.8
K	-	2
Compartment Size/ Size of production region	0.05	0.05
Domain size	1	
Location	0.025	-
Target location	0.975	

	Node X	Node Y
ω	0.3	2.8

	Node X	Node Y
ω	3	0.28

C

	Node X	Node Y	Inhibitor Z
ω	2	3	3.5
Compartment Size/ Size of production region	0.05	0.05	0.05
Domain size	1		
Target location	0.975		

	Node X	Node Y	Inhibitor Z
ω	2	3	0.35

	Node X	Node Y	Inhibitor Z
ω	0.2	3	3.5

	Node X	Node Y	Inhibitor Z
ω	2	0.3	3.5

D

	Node X	Node Y	Inhibitor Z
ω	1.7	3	3.5
Compartment Size/ Size of production region	0.05	0.05	0.05
Domain size	1		
Target location	0.975		

	Node X	Node Y	Inhibitor Z
ω	5	2.5	3.7

Figure 7

E

Node	X	Y
P <sup>T</sup>	6	Same as X
k <sup>b</sup>	100	-
k <sup>u</sup>	100	-
k <sup>t</sup>	0.1	0.1
k <sup>d</sup>	0.02	0.02
k <sup>2</sup>	10	100
k <sup>-2</sup>	100	100
r <sup>0</sup>	1.7	1.92
r <sup>TF</sup>	2E-04	-
r <sup>d</sup>	0.1	0.1
D	0.4	0.4

X and Y expressed from same template.  
Y as transcription factor.

Node	X	Z	Y
P <sup>T</sup>	6	10.5	Same as X
k <sup>b</sup>	100	-	-
k <sup>u</sup>	100	-	-
k <sup>t</sup>	0.1	0.1	-
k <sup>d</sup>	0.02	0.02	-
k <sup>2</sup>	10	100	-
k <sup>-2</sup>	100	100	-
r <sup>0</sup>	1.7	1.1	0.01
r <sup>TF</sup>	2E-04	-	-
r <sup>d</sup>	0.1	0.1	1
r <sup>RISC</sup>	20	-	-
D	0.4	0.4	0

	RISC
RISC <sup>Total</sup>	10
k <sup>b</sup>	0.1
k <sup>u</sup>	1

X and Y expressed from same template.  
Y mRNA activates RISC.  
Z as transcription factor.

Figure S1

A

Node	X
k <sub>1</sub>	4
K <sub>1</sub>	100
k <sub>2</sub>	100
K <sub>2</sub>	0.1
k <sub>d</sub>	0.1, 0.15, 0.2, 0.3

D

Node	X	Y
k	0.05	0.02
K	0.08	0.08
k <sub>d</sub>	0.02, 0.08, 0.4	

Figure S2

Node	X	Y
P <sup>T</sup>	4	8
k <sup>b</sup>	100	100
k <sup>u</sup>	100	100
k <sup>t</sup>	0.1	0.1
k <sup>d</sup>	0.02	0.02
k <sup>2</sup>	10	10
k <sup>-2</sup>	100	100
r <sup>0</sup>	1.7	1.3
r <sup>TF</sup>	2E-04	2E-04
r <sup>d</sup>	0.1	0.1
D	0.4	0.4
r <sub>const</sub>	-	-
L	0.1	

Figure S3

Node	X
k <sub>b</sub>	10
k <sub>u</sub>	10
P <sub>T</sub>	100
k <sub>d</sub>	0.01
D <sub>x</sub>	0.01

Table S1

Result	Justification
<b>Well mixed compartments</b>	
<b>Non-monotonic effects in simple motifs</b>	Analysis using simplified models (ignoring dimerisation in channel/ leak of dimer) demonstrates this behaviour. Computational results for the full model.
<b>Non-monotonic effects with feedback</b>	Building on the understanding gained from the simple motifs above. Computational results for the full model.
<b>Adaptation to spatial separation</b>	Analysis using monomeric regulation - clearly demonstrates the effect. Analysis extended to the full system with dimerisation. Computational results for the full system with dimerisation.
<b>Bistable motif.</b>	Analysis (including 1 and 2 parameter bifurcation analysis) using simplified model explains the qualitative trends. Computational results (including PDE equilibrium continuation) for the full model.
<b>Repressilator</b>	Computational results for two different sets of parameters - the original repressilator model parameter values (Biomodels page) and a set of values used in a cell-free realisation of the repressilator (Niederholtmeyer et al. 2015). Analogous results obtained for both sets of parameters.
<b>Resource sharing</b>	We incorporate sharing of RNAP by two nodes. Computational results for the full model. The basic effect of resource sharing shown here - biphasic response - has been demonstrated in other studies (Qian et al. 2017)
<b>Uniform Channel</b>	
<b>Non-monotonic effects</b>	Building on the understanding gained from well-mixed compartment, now including the effect of the boundary. Analysis of a single 'sender' compartment - analytical solution for a constant production of output and no dimerisation. Analytical solutions for (i) open boundaries with no degradation (ii) open boundaries with uniform degradation (iii) closed boundaries with uniform degradation.
<b>Symmetric locations</b>	Obtained using the above analytical solutions.
<b>Non-monotonic effect of varying diffusivity</b>	Obtained using the above analytical solutions.
<b>Basic effects of degradation</b>	Obtained using analytical solutions for a model without dimerisation.
<b>Localised bistable motif in uniform channel</b>	Analysis of a single node autocatalytic bistable motif (Gines et al. 2017) in (i) a 1-D domain with open boundaries and no degradation (ii) a 1-D domain with closed boundaries and uniform degradation. Computational results for the full PDE model, including numerical bifurcation analysis. Similar qualitative trends are observed for a single node, self-activating TX+TL motif. This is seen using numerical bifurcation analysis for the full PDE model.
<b>Localised oscillator in a uniform channel</b>	Analysis in the well-mixed configuration. Computational results for full PDE system in the 1-D channel. Similar qualitative trends across multiple oscillatory reaction systems, including (i) the activator-inhibitor TX+TL motif used in the study (ii) Rondelez' predator prey oscillator (using model) (iii) the Oregonator model (iv) the Brusselator model (iv) a chemical oscillator (Strogatz 1994)